One gene - two proteins: The C-terminus of the prototypical M2 muscarinic receptor localizes to the mitochondria

Irene Fasciani[a†], Francesco Petragnano[a†], Ziming Wang[b], Ruairidh Edwards[c], Narasimha Telegu[b], Ilaria Pietrantoni[a], Henrik Zauber[b], Mario Rossi[c], Ulrike Zabel[d], Marlies Grieben[b], Maria Eirini Terzenidou[c], Jacopo Di Gregorio[a], Cristina Pellegrini[a], Silvano Santini Jr[e], Anna Rita Taddei[f], Barbel Pöhl[b], Stefano Aringhieri[g], Gabriella Aloisi[a], Francesco Marampon[h], Alexandra Roman[b], Sebastian Diecke[b], Vincenzo Flati[a], Franco Giorgi[f], Fernanda Amicarelli[e], Andrew B. Tobin[c], Marco Scarselli[g], Kostas Tokatlidis[c], Martin J Lohse[b,d,i]*, Roberto Maggio[a]*, Paolo Annibale[b]*

[a] Department of Biotechnological and Applied Clinical Sciences, University of L'Aquila, 67100 L'Aquila, Italy.

[b]Max Delbrück Center for Molecular Medicine, 13125 Berlin, Germany.

[c]Centre for Translational Pharmacology, Institute of Molecular, Cell and Systems Biology, College of Medical, Veterinary and Life Sciences, University of Glasgow, G128QQ Glasgow, UK.

[d]Institute of Pharmacology and Toxicology, University of Wuerzburg, 97078 Wuerzburg, Germany.

[e]Department of Life, Health and Environmental Sciences, University of L'Aquila, 67100 L'Aquila, Italy.

[f]Section of Electron Microscopy, Great Equipment Center, University of Tuscia, Viterbo, Italy.

[g]Department of Translational Research and New Technology in Medicine, University of Pisa, 56126 Pisa, Italy.

[h]Department of Radiotherapy, University of Roma La Sapienza, 00151 Roma, Italy

[i] ISAR Bioscience Institute, 82152 Munich, Germany

[†] equal contribution

*email: m.lohse@mdc-berlin.de;

*email: roberto.maggio@univaq.it;

*email: paolo.annibale@mdc-berlin.de

Abstract

Muscarinic acetylcholine receptors are prototypical G protein-coupled receptors activated by the endogenous neurotransmitter acetylcholine. We show here that the carboxyl terminal fragment of the muscarinic M_2 receptor, containing the transmembrane regions VI and VII (M_2tail), is expressed by virtue of an internal ribosome entry site. The M_2tail fragment, whose expression is upregulated in cells undergoing integrated stress response, does not follow the normal route to the plasma membrane, but is almost exclusively sorted to mitochondria: here it controls oxygen consumption, cell proliferation and the formation of reactive oxygen species via reduction of oxidative phosphorylation. The expression of the carboxyl-terminal of a G protein-coupled receptor, capable of regulating mitochondrial function, constitutes a hitherto unknown mechanism that cells may use for controlling their metabolism under variable environmental conditions.

Muscarinic receptors include five structurally related receptors, belonging to class A of the G protein-coupled receptor (GPCR) family[1]. They are comprised of seven trans-membrane domains (TM domains I-VII) connected by intra and extracellular loops. Of these structural elements, the third intracellular (i3) domain is the one conferring a coupling specificity for G-proteins, β-arrestin recruitment and endocytic internalization [2]. However, only a small portion of the i3 loop is required for receptor function, and for this reason large deletions of this segment have no effect on receptor activation and internalization [3]. We previously showed that the M_2 receptor can be split at the level of the i3 loop into two segments, each behaving as an autonomous folding unit capable of targeting the plasma membrane and surprisingly reconstituting a physiologically active receptor when expressed together in transfected cells [4].

In eukaryotes, the most common mechanism of translation initiation is the cap-dependent process, which requires the interaction of several key proteins at the 5'-end (5′ cap) of mRNA molecules. However, in recent years, it has been demonstrated that the presence of internal ribosome entry site (IRES) sequences, which are common features of virus replication[5], can mediate cap independent translation of eukaryotic RNA(s) [6].

GPCRs are normally distributed at the plasma membrane, where, after activation by an agonist and coupling to G-protein, regulate a number of intracellular effectors. Nevertheless, non-canonical localizations of GPCRs have also been described, such as in endosomes [7], cell division compartments (centrosomes, spindle midzone and midbodies)[8], and mitochondria [9 10], underpinning non-traditional roles for this protein family.

Now, we have observed that the expression of the C-terminal domain of the M_2 muscarinic receptor, a region containing the TM regions VI and VII, occurs naturally by a cap-independent translation mechanism. We have further observed that the C-terminal domain of this receptor is strongly targeted to the cell mitochondria. Importantly, this mitochondrial targeting has functional ramifications since both cap-dependent mediated overexpression of the C-terminal domain alone, as well as cap-independent mediated translation starting from the mRNA of the full length M_2 receptor, resulted in a sizable reduction of oxidative phosphorylation.

In summary, this study reports the new observation that alternative reading of a receptor gene can give rise to a part of the receptor protein that serves an entirely different cellular function.

Results

Ligand binding and functional properties of M_2stop228.

To investigate and distinguish the functional roles of the two known N-terminal (TM1-5) and C-terminal (TM6-7) domains of the M_2 muscarinic receptor, we expressed C-terminally truncated variants of the receptor in COS-7 cells. We first observed that the M_2stop228, a receptor mutant bearing a stop codon at position 228, that is the beginning of the i3 loop (**Fig. 1a** and **Supplementary Fig. 1**), exhibited unexpected binding activity [11] albeit at a very low level of expression, i.e. 45 fmol/mg of protein. Both, the [^{3}H]NMS (N-methylscopolamine, an antagonist) K_D value, calculated from direct saturation experiments, and the IC_{50} values, calculated in competition experiments for the agonist carbachol, were in fact similar to those calculated for the wild type M_2 receptor (**Table 1**). Furthermore, the M_2stop228 receptor was found functionally active as it was capable to inhibit adenylyl cyclase [11] and increase ERK phosphorylation (**Supplementary Fig. 2b**), even though the extent of response was reduced if compared to the wild type M_2 receptors.

However, as previously shown [12], a receptor fragment with a stop codon in the i3 loop and devoid of the downstream sequence, called M_2trunk(1-283) (**Fig. 1b and Supplementary Fig. 1**), did not show any radio-ligand binding activity upon expression in COS-7 cells, despite it contained the first five trans-membrane regions of the wild type M_2 receptor (**Table 1**). Consistently, the first part until the stop 228 of M_2stop228, devoid of the downstream sequence M_2trunk(1-228), did not show any radio-ligand binding (**Table 1**).

These data strongly suggest that, for the M_2stop228 receptor to display binding and functional activities, the receptor sequence downstream of the stop codon (containing TMVI and VII) has to be translated and has to presumably interact with the first five TM regions of the M_2 receptor. This would mimic what was observed in the co-transfection experiments with the trunk and tail part of M_2 shown in **Table 1,** highlighting a recovery of the binding and downstream signaling ability of the N-terminal

(TM1-5) portion of the receptor, when expressed with the corresponding C-terminal (TM6-7) portion. This notion is graphically summarized in **Fig. 1b.**

That the C-terminal portion of the receptor can still be expressed despite the presence of stop codons in the initial part of the i3 loop was further confirmed by fusing an Enhanced Green Fluorescent Protein (EGFP) at the C terminus of the gene of the receptor mutants. While cells expressing the M_2-EGFP displayed the normal predominant membrane expression (**Fig. 1c**), cells expressing the M_2stop228 displayed a visible intracellular green fluorescence, as opposed to the receptor mutant M_2stop400, containing an in-frame stop codon in TMVI (**Fig. 1c**). Interestingly, the insertion of a frame shift, by adding a single nucleotide at position 1101 (M_2fr.sh.-EGFP, see **Supplementary Fig. 1)**, yielding an in-frame stop codon at position 370, still lead to formation of an EGFP labeled C-terminal fragment **Fig. 1c.** Since the EGFP is now out of the original reading frame, it can only be properly translated if a cap-independent translation initiates in frame with it.

This observation suggested that the stop codon should be localized in the i3 loop, for the receptor to be reconstituted, as confirmed by binding analysis of the additional receptor mutants shown in **Supplementary Fig. 2a** **and** **Supplementary Table 1**, pointing to the third in-frame methionine of the i3l loop (M368) as the most likely site for the initiation of translation of the C-terminal domain.

Notably, similar results were also obtained by inserting a stop codon in the i3 loop of the related muscarinic M_3 receptor at position 273, M_3stop273 (for details see **Supplementary Fig. 1** and **Supplementary Table 2 and 3**), thus indicating that this phenomenon is not restricted solely to the M_2 receptor, but may be common among at least some members of the GPCR superfamily.

Immunodetection of the M_2 carboxyl terminal fragment

To assess the pattern of proteins generated from the constructs containing the mutations reported in **Fig. 1a**, HEK293 cells were transfected with the wild type M_2 receptor, the C-terminal fragment

starting at the third in-frame methionine M_2tail(368-466), a mutant of the M_2 receptor with the M368A mutation and finally the M_2stop400, c-terminally fused to a myc-tag for immune detection. The constructs were expressed in a bicistronic vector backbone, allowing also the expression of the red fluorescent protein mRuby2, as a fluorescent reporter to verify comparable expression levels. The constructs were resolved by SDS-PAGE and assayed by Western blotting with an anti-myc antibody. **Fig. 2a**, illustrates the protein products observed when expressing the M_2 receptor. The full-length receptor, including commonly observed higher order oligomers, were observed at about ~75 kDa [13]. However, the M_2 receptor lane displayed also two clear bands running at ~20 and ~15 kDa. The molecular weight of these bands is equivalent in size to what would be expected for a M_2 carboxyl terminal fragment starting at the third in-frame start codon (ATG 368) of the M_2 or M_2stop228 construct (~15kDa), as predicted by binding experiments (**Supplementary Table 2**). Indeed, these two bands match those observed in the lane containing lysates of cells expressing the M_2tail(368-466). Interestingly, in the M_2M368A the heavier of these two bands disappeared, whereas the 15 kDa band displayed a reduced intensity. Finally, the control construct M_2stop400 did not exhibit any band, similarly to the untransfected cells, meaning that if a protein is translated starting from the third in frame methionine (368) of the i3 loop, it would be terminated after 32 aminoacids (at stop 400), hence losing the myc tag at the C-terminus (**Fig. 2a**).

Similar results to those obtained in HEK293 cells were also obtained by transfecting myc-tagged constructs in COS-7 cells (**Supplementary Figure 4**).

We then tested whether a similar phenomenon, namely the translation of the C-terminal portion of the M_2 receptor, could be observed endogenously in physiological settings. We therefore prepared protein extracts from heart, brain and spleen tissues from a line of knock-in mice (see Methods), designed to have expression of a Chrm2/tdtomato fusion protein driven by the endogenous M_2 muscarinic acetylcholine receptor promoter/enhancer sequences. The heart and brain are known to express sizable levels of the M_2 receptor, whereas the spleen, where no expression of the M_2 receptor is reported in the proteomic databases, was used as a negative control.

The use of a transgene tag was necessary, since antibody against the M_2 receptor are notoriously ineffective, in particular when targeted at the C-terminal portion of the receptor. Instead, the tdtomato fluorescent protein can be targeted by a specific polyclonal antibody, as shown by the Western blot displayed in **Fig. 2b**. As expected, the full-length receptor was observed at ~120 kDa (tdtomato has a molecular weight of ~55 kDa). Notably, both in the heart and brain from knock-in animals a specific bands doublet was observed at ~75 kDa, that corresponds to the molecular weight expected from the sum of the tail fragments, also observed in the blot of **Fig. 2a,** to the molecular weight of tdtomato.

Testing bicistronic constructs for the presence of an IRES.

To explain the translation of the carboxyl terminal fragment of the M_2 receptor, a mechanism enabling a cap-independent initiation of protein synthesis should be hypothesized [5,6]. Accordingly, an IRES should be found downstream of the artificial stop codon 228 and preceding the third in-frame methionine (codon 368) of the i3 loop. To test this hypothesis, we prepared a construct in which the i3 loop of M_2, from nucleotide 685 (a.a. 228) to nucleotide 1101 (a.a. 368), was inserted between the two fluorescent proteins Sirius and EGFP (**Fig. 3a**). This construct, named Sirius-M_2i3(417n)-EGFP, would translate Sirius according to the classical cap-dependent mechanism, and, at the same time, it would drive EGFP translation only if the M_2i3 loop contains an IRES sequence, acting as a bicistronic expression cassette. Several cell lines were transfected with this construct. HEK293 cells appeared positive for both the blue and green fluorescence, as shown in the insert of **Fig. 3a**. COS-7, SHSY-5Y, CHO and HeLa cells were also all positive for the blue and green fluorescence (**Supplementary Fig. 5a**). Similar results were observed when 558 nucleotides from the i3 loop of the M_3 receptor were inserted in the bicistronic construct (**Supplementary Fig. 5b and c**), underlining that cap-independent translation is a more general feature of muscarinic receptor mRNAs than previously thought.

To rule out the possibility that the functional properties of the Sirius-M_2i3(417n)-EGFP construct could be accounted for by read-through and termination-re-initiation mechanisms, a hairpin loop was

inserted after the stop codon of the Sirius protein. The construct Sirius-H-M_2i3(417n)-EGFP showed only a slight reduction of the EGFP fluorescence (85 ± 8% of the value measured for the Sirius-M_2i3(417n)-EGFP plasmid) (**Fig. 3a**). In contrast the Sirius-H-EGFP plasmid, where the entire M_2i3 loop after the Sirius was removed, showed a negligible EGFP/Sirius ratio, underlining the importance of the i3 loop for the EGFP expression (**Fig. 3a**). Notably, when the hairpin was inserted within the i3 loop of the full length M_2 receptor, it was still possible to observe GFP fluorescence (**Supplementary Fig. 5d)**.

In order to narrow down the position of the IRES sequence within the M_2i3 loop, the i3 loop sequences of five related GPCRs, i.e. the five muscarinic receptors, were compared. Only the alignment of the last portion of the M_2 i3 loop (from nucleotide 1072 to 1104) with regions adjacent to the second (M_1), fourth (M_3 and M_4) and first (M_5) in-frame ATGs, clearly showed that some nucleotide residues are conserved (**Supplementary Fig. 6**). On the basis of this preliminary observation, the M_2 i3 loop was divided in three parts and the resulting nucleotide sequences, 685-699, 685-1071 and 685-699/1072-1101, were inserted downstream of the hairpin loop in three different constructs.

EGFP fluorescence was not significantly rescued upon insertion of the first 15 nucleotides (685-699) of the i3 loop after the hairpin, nor by the subsequent 372 nucleotides (685-1071). However, when the last portion of the M_2 i3 loop was inserted in the construct after the Hairpin, leading to Sirius-H-M_2i3(15n/30n)-EGFP, 110 ± 5% of the value measured for the Sirius-M_2i3(417n)-EGFP plasmid was recovered (**Fig. 3a**). This was in line with the results of binding experiments from the muscarinic M_2 receptor (**see Supplementary results and Supplementary Table 1**). These data suggest that the M_2 i3 loop is essential for EGFP to be expressed and that an IRES, present within the sequence, controls its expression.

These results strongly suggest that the IRES is located in a region of the i3 loop sequence immediately upstream of the third methionine (M368) (see **Fig. 1a**). This conclusion is also supported by the finding that when each of the three in frame ATG codons after the stop codon 228 of the M_2stop228 were mutated to an additional stop codon, only the suppression of the third ATG (368) proved capable

of completely abolishing [^{3}H]NMS binding (**Supplementary results** and **Supplementary Fig. 1 and Supplementary Table 1**). These binding results could also account for read-through and termination-reinitiation. In fact, if these mechanisms were responsible for translation of the C-terminal of the M_2stop228, suppression of the first ATG would have abolished the binding. Furthermore, the origin of the carboxyl terminal fragment of M_2 at the third in-frame methionine (M368) is also supported by the fact that a mutant M_2-M368A-myc, in which the methionine (368) was substituted with an alanine, expressed a negligible amount of the M_2tail fragment as compared to the wild type M_2-myc receptor (**Fig. 2a**).

Based on this evidence, we mutated the conserved residues highlighted in yellow in **Supplementary Fig. 6,** in order to check for their relevance in recruiting the ribosome on the M_2 i3 loop sequence, as shown in **Fig. 3b**. As discussed in detail in the **Supplementary Results**, we found that the four nucleotides AAGA1090-1093 next to the methionine 368 play a pivotal role in recruiting the ribosome on the M_2 mRNA and in translating the M_2tail fragment.

Localization of the transiently transfected M_2-Muscarinic Receptor C-terminal fragment in living cells.

After having established how the expression of the M_2 C-terminal domain is regulated, we went on to study the role it might play in the cell. For this purpose, M_2tail(368-466) fused to the fluorescent protein EGFP was expressed in HEK293 cells. Confocal microscopy demonstrated a striking mitochondrial localization of the M_2tail(368-466)-EGFP construct (**Fig. 4a**). This was confirmed by co-staining of HEK293 cells with a conventional mitochondrial stain (Mitotracker Deep Red) and by co-expressing M_2tail(368-466)-EGFP with Tom20-mCherry, a fluorescently labeled construct targeted to the outer mitochondrial membrane (**Supplementary Fig. 7a**). The observed mitochondrial localization of the M_2tail(368-466)-EGFP, appeared in stark contrast to the canonical cellular localization of the M_2 receptor, as shown in **Fig. 4b** where the M_2 muscarinic receptor was C-

terminally labeled with the red fluorescent protein mRuby2. Interestingly, very little expression of M_2tail(368-466)-EGFP was observed on the plasma membrane, as confirmed by fluorescence correlation spectroscopy[14] experiments aimed at assessing the potential interaction with the full-length receptor (**Supplementary Fig. 7b-d**). By contrast, when the M_2tail(368-466)-EGFP was co-expressed with M_2stop228, a modest localization could eventually be detected also on the cell membrane, suggesting a chaperon activity of the M_2 N-terminal (M_2trunk) (**Supplementary Fig. 7e-g**) and hence explaining the [^{3}H]NMS binding observed in cells transfected with M_2stop228 and M_2trunk(1-228) + M_2tail(368-466) (**Table 1**). Likewise, constructs such as M_2tail(368-466)-mRuby2 (a red monomeric fluorescent protein) and M_2tail(368-466)-tdTomato (a tandem-dimer red fluorescent protein) also displayed mitochondrial localization (**Supplementary Fig. 7h-i**), ruling out a possible bias due to the fluorophore used.

Localization of the IRES driven M_2 carboxyl terminal fragment within living cells.

We sought to express the C-terminal tail of the M_2 receptor under the control of the IRES rather than a viral promoter, to further exclude the possibility that the observed localization of the M_2 carboxyl terminal fragment was due to overexpression of the construct. HEK293 cells were transfected with a mega construct M_2-mRuby2-STOP-M_2-i3-tail-EGFP which contains the full wild type M_2 receptor, mRuby2-labeled at the C-terminal, fused to the C-terminal part of the M_2 receptor starting at nucleotide 685 of the i3 loop, following the stop codon of mRuby2, and ending with a C-terminal EGFP sequence. Through this experimental strategy, the expression of M_2tail(368-466)-EGFP is regulated by the IRES, and the mechanism of C-terminal fragment production is therefore physiological. The expression of EGFP confirmed that the *in vivo* production of the M_2tail(368-466) is regulated by the IRES within the i3 loop. In addition, the processed receptor fragment was eventually observed to be predominantly confined to the cytosol and the mitochondrial network (**Fig. 4c**).

Notably, when the M_2-EGFP fusion protein was expressed and the cells were co-stained with Mitotracker, a faint EGFP signal was also observed in the mitochondrial regions (**Supplementary Fig. 8a**), although the expression of the full-length receptor masks this effect and makes quantification difficult. On the other hand, **Fig. 4d** shows that, when the M_2fr.sh-EGFP mutant was expressed in HEK293 cells, the IRES generated C-terminal fragment of the M_2 receptor still localized to the mitochondria. As mentioned above, in this construct the masking effect of the EGFP fused to the full length receptor is removed. Similar mitochondrial localization was also observed when HEK293 cells were transfected with M_2fr.sh-mRuby2 (**Supplementary Fig. 8b**), ruling out possible effects due to the specific fluorophore used as a tag. Similar findings were also obtained in COS-7 cells (**Supplementary Fig. 8c**).

Mitochondrial import of the C-terminal fragment of the M_2 receptor was further verified by immunoblotting of protein extracts from purified mitochondria of HEK293 cells transfected with myc-tagged M_2 receptor, M_2tail(368-466) and M_2M368A. **Fig. 4e** shows that in purified mitochondria (unlike in the cytosolic and microsomal supernatants originating from the purification process, **Supplementary Fig. 8d**), only the protein bands associated to the M_2 C-terminal fragment was visible.

Notably, no mitochondrial import whatsoever was visible for the M_2M368A, confirming that the third in frame methionine in the third i3 loop of the M_2 receptor is necessary for the C-terminal fragment production and its localization in the mitochondria.

A consistent result was observed when mitochondria were purified from the heart and spleen of the Chrm2/tdtomato mice **Fig. 4f** (the cytosolic fraction is shown in **Supplementary Fig. 8e**). A band at ~75 kDa, matching the molecular weight of the M_2 C-terminal domain, was clearly visible. The band runs together with what is likely a degradation product, below, and a higher order aggregate above, at ~110 kDa. We conclusively confirmed that this is the fingerprint associated to the M_2 C-terminal fragment, by purifying mitochondria from HEK293 cells expressing the construct M_2tail(368-466)-tdtomato. **Fig. 4g** (cytosolic fraction is shown in **Supplementary Fig. 8e**) shows that the observed

protein bands in the blot from the cell extracts matched closely the bands observed in mitochondria from mice tissues, including not only the ~75 kDa bona-fide M_2tail band, but also the lower and higher molecular weight bands.

Mitochondrial localization of the M_2tail originating from the wild type M_2 receptor was finally confirmed by relative abundance estimates of EGFP and M_2 receptor from Parallel Reaction Monitoring (PRM) based mass spectrometry measurements **Supplementary Fig. 9**. Samples were prepared by preparing mitochondrial and cytosolic fractions (**Methods**) from HEK293 cells, expressing M_2-EGFP and a set of control constructs, including M_2tail-EGFP, pmito-EGFP (an EGFP fused to the mitochondrial leading sequence of the cytochrome c oxidase subunit 8A (COX8A)), lifeact-EGFP (a cytosolic protein) and Epidermal Growth Factor receptor fused to EGFP (EGF-EGFP). A 15-aminoacid long peptide originating from EGFP was screened. The bands intensities of the cytosolic fraction, were normalized to consider both the overall loading variability as well as the relative transfection efficiencies among the samples. Notably, we observed a mitochondrial enrichment of the EGFP derived peptide as well the receptor-specific peptide originating from the M_2 receptor, in agreement with the positive mitochondrial localization control.

Mechanism of import of the M_2 carboxyl terminal fragment into the mitochondria and localization within the organelle

In order to gain further insight into the dynamics of the M_2 C-terminal fragment import within the mitochondria, we first monitored the kinetics of colocalization between mitochondria and EGFP in cells transfected with M_2tail(368-466)-EGFP. **Fig. 4h** highlights the expression of the M_2tail(368-466)-EGFP during four hours, starting at 5h after transfection. The construct was found initially expressed in the perinuclear region, likely the ER, indicating that at least the initial step of the anterograde transport of the M_2tail(368-466)-EGFP is the same as for the full length receptor[15]. At this time (5h from transfection), almost no colocalization with the Mitotracker-stained mitochondria was visible. However, within 1 hour (6h), the colocalization level increased significantly, and the M_2

C-terminal fragment was either found in the cytosol or in the mitochondria. After 4 hours (9h from transfection) the colocalization at the mitochondria was well visible. We quantified the colocalization level over time using the Manders' coefficients. The resulting chart, indicates that almost half of the mitochondrial import occurred within 1 hour.

This value is qualitatively in agreement with what we observed using an in-vitro assay to determine the import of the M_2 carboxyl terminal into isolated mitochondria (see Methods). To this end, we used mitochondria form S. cerevisiae, which are a robust and well-studied system for protein import assays. **Supplementary Fig. 10a** shows the autoradiography experiment of isolated, intact, mitochondria incubated with 35S-labelled full length muscarinic M_2 receptor or M_2tail(368-466), made using a reticulocyte in vitro translation system. The data show that the full-length receptor, (running at ~55 kDa in this assay as highlighted by the 5% control lane) was not imported into mitochondria. On the other hand, the M_2tail(368-466) (running as a doublet at 11 and 16 kDa) displayed a striking mitochondrial import already after 5 minutes and increasing over time, up to 30 minutes. These data suggest that the lower band arises from a processing and cleavage step occurring inside the mitochondria, as also observed in the Western blots of **Fig. 4e** in HEK293 cells. **Supplementary Fig. 10b** shows that the import does not depend on transporters of the outer membrane Tom5, Tom6, Tom7 and Tom70. On the other hand, the import of an inner membrane protein, the ADP/ATP carrier (AAC), used here as a control, depends on Tom70. Upon extraction with carbonate (last two lanes in the top panel), most of M_2tail(368-466) was found in the pellet, and therefore presumably integrated in a membrane. Blue native analysis suggests that the mitochondrially imported M_2tail(368-466) is not a monomer but rather it is part of a larger complex of approximately 180 kDa **Supplementary Fig. 10c.**

All together these data suggest that the import of the M_2tail(368-466) leads to its localization in one of the mitochondrial membranes, to form a complex with other native mitochondrial proteins.

In order to discriminate if the construct is on the outer or inner mitochondrial membrane, we set up a fluorescence assay based upon the self-complementing split GFP protein technique [16]. HEK293 cells were transfected with two constructs: M_2tail(368-466)-GFP11, in which a short 16 amino acids peptide of GFP was fused at the C-terminus of M_2tail(368-466), and mito-GFP1-10, in which the COX8A was N-terminally fused to the other GFP fragment containing the remaining 10 beta strands (See Methods). **Supplementary Figure 10d** shows the successful recombination of the two within the mitochondrial matrix. We then applied this approach to the full length M_2 receptor, by generating the M_2-GFP11 construct and by transfecting it in HEK293 cells. **Fig. 4i** shows a green signal from the recombined GFP visible in the mitochondria. All together these data suggest that the M_2 C-terminal fragment is localized in the inner mitochondrial membrane, with its own C-terminal domain facing the matrix.

This interpretation appears to be confirmed in cells expressing the M_2stop228-myc receptor and examined by electron microscopy (**Supplementary Fig. 10e**) after immune-gold labelling. As shown in **Supplementary Fig. 10f-g**, gold particles were observed only in mitochondria, and at this stage they appeared localized either to the mitochondrial matrix or to the lumen of the cristae, as highlighted by the detailed views of **Supplementary Fig. 10h-k.**.

Influence of the M_2-muscarinic receptor C-terminal fragment on cell metabolism

The next step of our investigation concerned the obvious question about the functional effects, if any, that the observed localization of the M_2 C-terminal fragment might have on the mitochondrial activity, and -more generally- on the energy metabolism of the cell. To investigate this aspect, we measured the extent of oxygen consumption in COS-7 cells expressing M_2-EGFP, M_2tail(368-466)-EGFP or the sole EGFP as a control. Initially, we normalized the expression of the three proteins respect to the amount of EGFP expressed in the cells, then the metabolic functions were assayed on a Seahorse instrument using cells transfected with normalized amounts of plasmids **(Fig. 5a)**.

Our data did not show a significant difference in total oxygen consumption capacity between cells transfected with cytosolic EGFP and the untransfected control. However, a significant decrease of oxygen consumption was found in cells transfected with M_2-EGFP and even more so with M_2tail(368-466)-EGFP (**Fig. 5a**). Notably, the basal oxygen consumption rate (OCR), in starvation-stress conditions, was profoundly decreased in M_2tail(368-466) cells and to a smaller extent in M_2 cells compared to EGFP and empty control cells (see also the time-course in **Supplementary Fig. 11a)**. These results are in line with what was observed using a Clarke-type oxygen electrode (**Supplementary results and Supplementary Fig. 11b and 11c**).

A cell apoptosis assay, based on the detection of activated caspase-3 [17], did not show substantial differences among the tested mutants (**Supplementary Fig. 11d**). The overexposed western blot showed a tiny amount of activated caspase-3 in most of the transfected COS-7 cells, indicating that the expression of M_2tail(368-466) in mitochondria, in agreement with the qualitative post-starvation data shown in **Supplementary Fig. 11e**, does not induce fragmentation of the mitochondrial network and cell apoptosis.

To test whether the C-terminal-M_2 fragment effects on mitochondrial oxygen consumption could alter the production of Reactive Oxygen Species (ROS), the measurements were combined in a single cell assay. Remarkably, ROS production (assayed using a fluorescence readout kit, where the fluorochrome becomes activated in contact with oxidized species, as shown in red in **Fig. 5b**) was clearly reduced within and in proximity of mitochondria of cells expressing a high level of the M_2tail(368-466). By regrouping individual mitochondria in classes according to the level of the ROS marker expression, an actual inverse correlation between the amount of receptor fragment (Green Fluorescence) and the production of ROS (Red Fluorescence) was revealed.

Cell growth was also found to be affected depending on which of the constructs was transfected. Notably, transfection of HEK293 cells with the wild type M_2 receptor reduced significantly cell growth compared to the control, whereas cells transfected with the mutant M_2M368A, whose expression of the M_2 C-terminal fragment is very low, if any, and not in the mitochondria (**Fig. 5c**),

displayed a significantly higher growth. Notably, the cells were also exposed to the M_2 antagonist atropine, in order to exclude effects on cell growth and proliferation due to the canonical receptor signaling. Comparable results were observed when COS-7 cells were transfected with the indicated M_2 receptor mutants (**Supplementary Fig. 11f).**

Cell stress upregulates M_2 C-terminal expression and mitochondrial localization

Stressed cells attenuate their translational activity via phosphorylation of the initiation factor eIF2α. However, certain mRNAs may be insensitive to eIF2α phosphorylation level if their translation is regulated by IRES. Under these conditions their expression is bound to increase rather than to attenuate [18,19].

Therefore, COS-7 cells were transfected with the Sirius-M_2i3(417n)-EGFP construct and stressed by starvation for three hours by replacing the culture medium with HBSS or PBS. During this time interval, the green fluorescence was seen to gradually increase up to 1.4 times the basal level observed in HBSS-starved cells and 3.5 times for PBS-starved cells (**Fig. 5d**), further confirming that the C-terminal fragment expression is upregulated in response to stress conditions such as cell starvation. The same experiment was reproduced on single cells, displaying an increase of the average EGFP/Sirius ratio upon HBSS starvation in HEK293 cells (**Fig. 5e)**. This effect could be observed also by looking at the relative intensity of the M_2 C-terminal fragment band with respect to the full-length receptor band, upon serum starvation of HEK293 cells (**Fig. 5f)**.

We further used the split GFP complementation assay to emphasize the importance of stress in the pattern of expression of the M_2 gene. HEK293 cells were co-transfected with M_2-GFP11 and Mito-GFP1-10. HEK293 cells grown in culture medium predominantly expressed the full M_2 receptor protein (**Fig. 5g**). The green fluorescence detected in the plasma membrane could be explained with the chaperoning effect of M_2-GFP11 on Mito-GFP1-10 before its sorting to the mitochondria. In sharp contrast, when HEK293 cells were first transfected with Mito-GFP1-10 and, 24h later, transfected

with M_2-GFP11 followed by a 6 h starvation in HBSS, the pattern of expression changed drastically. IRES mediated translation of the M_2tail(368-466) fragment led to a predominantly mitochondrial green fluorescence signal of the complemented GFP (**Fig. 5g**). These results are in line with our observation that the IRES mediated C-terminal fragment localization to the mitochondria in cells expressing the mega construct *M_2-mRuby2-STOP-M_2-i3-tail-EGFP* was enhanced upon cell starvation, and drastically reduced upon mutation of the M368 (**Supplementary Figure 12** and **Supplementary Methods**).

This observation was also supported by the lack of complementation of M_2tail-GFP11 with GFP1-10 when this last fragment was N-terminally fused to the targeting sequence of SMAC, a protein expressed in the mitochondrial intermembrane space [20] (**Supplementary Fig. 13c**).

Mutation of the M368A via Crispr/Cas9 affects cell growth and oxygen consumption rates in hiPSCs

We finally asked the question of what would be the effect of abolishing the translocation of the M_2 C-terminal fragment to the mitochondria, in a physiological, entirely label-free setting. To reach this goal we genetically engineered (see Methods) human induced pluripotent stem cell (hiPSC), to incorporate in both alleles of the M_2 gene the M368A mutation, that, based on our data, should be sufficient to significantly impair the M_2 C-terminal production and mitochondrial translocation. Wild type and M368A hiPSCs were cultured in pluripotency maintaining medium, and subsequently undirectedly differentiated upon exposure for seven days to DMEM-F12 medium, as described in the Methods. **Fig. 5h** shows confocal micrographs for wild type and M368A hiPSCs cultured in E8 medium respectively. The M368A hiPSCs displayed a mildly more extended phenotype. We shall note here that the M_2 receptor has been found to be expressed in PSCs lines, and it has been shown to play a role in stem cell differentiation [21,22]. In this context, however, we were not interested in the canonical signaling of the receptor, and all experiments were performed with a saturating concentration of atropine, to block any activity of the receptor. We then evaluated cell proliferation,

observing a significant increase in the proliferation of the M368A clone 72h after seeding **Fig. 5i**. The observation of an increased proliferation of the cells harboring the mutation that impairs the production and localization of the C-terminal fragment in the mitochondria, suggests that the same effect is at play here, as observed in the overexpression system (**Fig. 5a,b,c**). These results are supported by extracellular oxygen consumption assays performed, for both hiPSCs and differentiated hiPSCs (**Fig. 5j).** Our data suggest that the M368A cells indeed display an accelerated oxygen consumption rate, and that this effect increases as the cell progressively differentiates.

For comparison, the assay was also carried on HEK293 overexpressing the wild type M_2 receptor and the mutant M_2M368A (**Supplementary Fig. 11g)**. We could observe with this assay a reduced oxygen consumption of the wild type M_2 receptor compared to untransfected cells, in line with what observed in **Fig. 5a** and an increased oxygen consumption of the M_2M368A expressing cells, in line with what observed for the hiPSCs.

Discussion

Over the last 10 years, growing evidence has accumulated indicating that, other than at the plasma membrane, GPCRs can be functional and signal also at other cellular locations. These locations can be associated to their canonical trafficking pathways (such as sorting vesicles and endosomes)[23], but also to non-canonical locations, such as the nucleus, the nuclear membrane, the Golgi apparatus and the mitochondria (reviewed in Jong et al. BPJ 2018 [24]). Some of these locations are surprising, since many ligands are non-membrane permeable, and it is still debated how they can reach their target receptors at such intracellular locations.

Interestingly, the specific localization of these receptors appears to go hand in hand with a specific function. In these cases, activation/inhibition of mitochondrially localized GPCRs have been shown to specifically affect the organelle function, ranging from oxygen consumption rates to Ca^{2+} handling and even to apoptosis. Notably Benárd et al [25] showed that the CB_1R on the outer mitochondrial membranes affects neuronal energy metabolism; Suofu et al. [10] demonstrated that activation of the MT_1R by a mitochondrial melatonin pool can affect cytochrome C release. This is particularly interesting, since cytosolic cAMP does not appear to be able to activate mitochondrial PKA, and hence a mitochondrially localized GPCR signalosome appears to be required to enable such downstream signaling cascade [26].

However, other non-canonical mechanisms are also possible for the regulation of mitochondrial function. It is well known that GPCRs are subject to interindividual variability, arising, for example, from mRNA alternative splicing (i.e. the process which allows the recombination of exons) which leads to different isoforms which may present distinct signaling and localization properties [27]. Receptor variants with different functional and localization properties may also occur due to other processes. For example, our comprehension of eukaryotic translational regulation is facing a rapid

expansion, as exemplified by the observation that small open reading frames (smORFs), also within lncRNAs, are an important class of genes, oftentimes with mitochondrial localization[28].

In this study, for the first time, we provide evidence that an IRES sequence drives expression of a membrane receptor fragment and acts as a regulator of its expression levels and function. IRES sequences are distinct regions of the mRNAs that are capable of recruiting ribosomes in the proximity of an internal initiation codon and translate transcripts in a cap-independent manner [5,6,29-31]. Here, we show that an IRES sequence is located within the third intracellular loop of the M_2 muscarinic receptor, where it plays a crucial role in regulating the expression of its carboxy-terminal domain, which we identified as M_2tail(368-466).

We assessed the IRES-driven expression of the C-terminal fragment through a broad set of constructs, meant to exclude alternative synthesis mechanisms such as stop-codon read-through, and a diversified palette of techniques. Radioligand binding data (**Table 1**) pointed to the necessity of the C-terminal fragment synthesis, in order to explain the observed downstream signaling in mutants carrying a stop codon in the initial portion of the i3loop of the M_2 receptor, upstream of M368. Fluorescence microscopy allowed us visualizing the production of the EGFP-tagged C-terminal fragment in these receptor mutants (**Fig. 1d**). We further detected its production by Western blotting on protein extracts from heart and brain tissues from knock-in mice carrying a C-terminally tagged M_2 receptor (tdtomato) and under the control of the endogenous promoter/enhancer sequences (**Fig. 2c**).

Mutagenesis of key residues within the i3 loop of the M_2 receptor allowed us to pinpoint the 3rd in-frame Methionine as the most likely candidate for the beginning of the cap-independent translation (**Fig. 3**). This observation appears to be supported by the observation of a peak in ribosome coverage around the M368, seen in ribosome profiling databases (as reviewed in Ingolia et al.[32]), and

particularly prominent in those from left ventricle cardiomyocytes, where M_2 receptor expression is known to be abundant[28].

To our surprise, in contrast to the plasma membrane localization of the wild type, full length M_2 receptor, the C-terminal fragment was localized mostly in mitochondria. This localization occurred markedly when overexpressing the C-terminal fragment M_2tail(368-466), but could be also clearly detected when the C-terminal fragment was expressed under the control of the IRES sequence of the full length receptor (**Fig. 4 c,d**).

We devised several strategies to detect the localization of the IRES-driven fragment in the mitochondria by avoiding the cell-wide background signal from the full-length receptor. **Fig. 4c,d** show two prominent examples, namely relying on spectrally unmixing the two components, or by sending out of frame the EGFP at the C-terminus of the full-length receptor. By studying mitochondria purified from HEK293 cells we could confirm that mutation of the M368, that we identified as the starting point of the IRES-mediated translation, is sufficient to suppress any mitochondrial targeting of the M_2 C-terminal fragment, and most likely, its synthesis altogether (**Fig. 4e**).

We then addressed the mechanism of mitochondrial import of the C-terminal fragment and its localization within the organelle. Our data, originating both from live cell import kinetics (**Fig.4h**) as well as from in-vitro import into isolated mitochondria (**Supplementary Fig. 10**), support the notion that the fragment becomes rapidly imported into mitochondria following translation in the cytosol. Once inside the mitochondria, it undergoes processing leading to the appearance of a lower molecular weight band, observed both in Western blots from whole cell and mice tissue protein extracts, as well as from purified mitochondria. The fragment is found predominantly in a carbonate-insoluble fraction, i.e. a membrane, and it appears to form a high molecular weight complex of ~180 kDa with other mitochondrial proteins (**Supplementary Fig. 10c**).

Fluorescence complementation assays (**Fig. 4i**) and electron microscopy (**Supplementary Fig. 10d**) suggest that the M_2 C-terminal fragment predominantly resides in the inner mitochondrial membrane, with its own C-terminal domain exposed towards the matrix. Future work should clarify the precise import pathway.

Most importantly, our data show that mitochondrial oxygen consumption was reduced by the M_2tail(368-466) (**Fig. 5a,b**), and also cell proliferation was affected (**Fig. 5c**). Under integrated stress response, namely aminoacid starvation, IRES-mediated production of the C-terminal fragment was increased (**Fig. 5d-g**). On these bases, the M_2tail might be needed in mitochondria as a means to reduce mitochondrial basal oxygen consumption and ATP-linked respiration. An important consequence of reduced respiration is the lower level of ROS produced in mitochondria, as we observed in agreement with this hypothesis.

This observation was confirmed in physiological, label-free conditions, by genetically editing human induced pluripotent stem cells in order to induce the M368A mutation in the gene of the M_2 receptor. Increase of cell proliferation of this clone compared to its wild type counterpart, together with an increase of oxygen consumption rates (**Fig. 5i-j**), corroborates our hypothesis that the M_2 C-terminal fragment reduces oxygen consumption upon reaching the mitochondria. The effect was further amplified when the cells were undirectedly differentiated, and it was consistent with the shift of the cell phenotype towards oxidative phosphorylation[33].

The mechanism by which the M_2tail(368-466) may reduce oxygen consumption in mitochondria and its meaning needs to be further explored. Nonetheless, since ROS production is implicated in the pathogenesis of several diseases[34], we would propose the hypothesis that increased localization of the M_2 C-terminal fragment in mitochondria, as it occurs under integrated stress response, might have protective effects.

In broader terms, protection of mitochondria by unconventional import mechanisms to allow localization within the organelle of specific proteins has been previously observed for cells that undergo stress conditions [35]. The mechanism of IRES-dependent modulation of translation and consequent mitochondrial targeting of certain translation products may provide another means of a generic cellular response to overcome different types of stress by modulating the mitochondrial proteome and adjusting the mitochondrial bioenergetic state.

Tables, Figures and Supplementary Tables and Figures

Table 1. Radioligand binding and activation properties of M_2 receptor mutants. Binding properties and inhibition of forskolin stimulated adenylyl cyclase by M_2, M_2stop228 and the co-transfected M_2trunk(1-283)/M_2tail(M-281-466) and M_2trunk(1-228)/M_2tail(368-466). Untransfected COS-7 cells did not show any [^{3}H]NMS specific binding. N.B. = no specific [^{3}H]NMS binding.

Binding data				Adenylyl cyclase inhibition assay	
Receptor	Bmax (fmol/mg)	[^{3}H]NMS KD (pM)	Carbachol IC50 (µM)	Carbachol EC50 (µM)	Maximum inhibition of forskolin stimulated cAMP accumulation (%)
M_2	980 ± 60	62 ± 7	2.1 ± 0.6	0.04 ± 0.01	53 ± 5
M_2trunk(1-283)	N.B.				
M_2trunk(1-228)	N.B.				
M_2stop228	45 ± 2	70 ± 10	1.8 ± 0.4	0.13 ± 0.02	27 ± 3
M_2trunk(1-283) +M_2tail(M-281-466)	480 ± 20	79 ± 10	0.7 ± 0.2	0.15 ± 0.03	37 ± 4
M_2trunk(1-228) +M_2tail(368-466)	70 ± 10	72 ± 8	0.6 ± 0.2	0.17 ± 0.03	29 ± 4

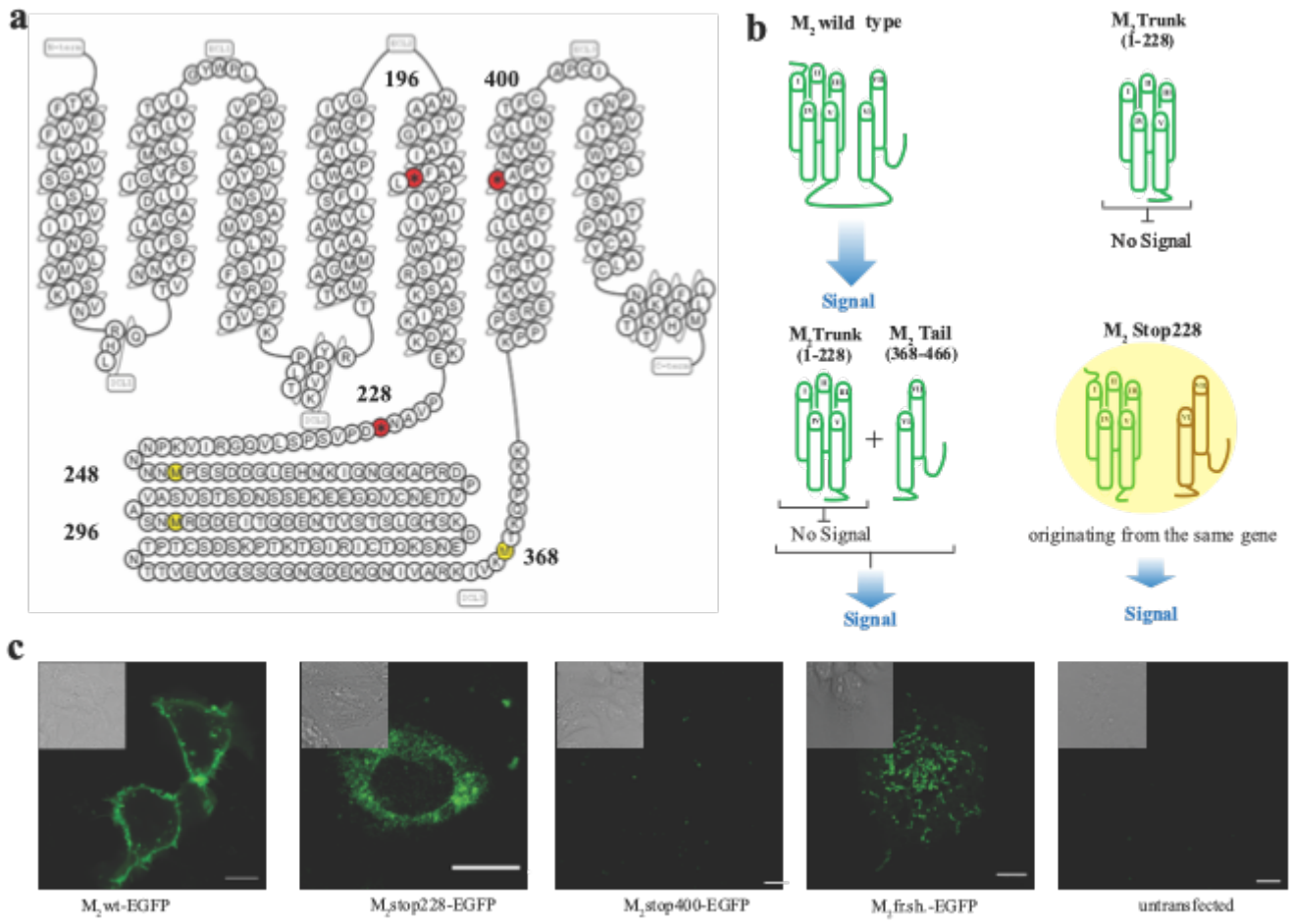

Fig. 1. Mutations of the M_2 receptor confer unexpected functional and localization properties. **a**, Snake-like plot of the human muscarinic M_2 receptor: in red are indicated the aminoacids substituted with stop codons in the mutants: M_2stop196, M_2stop228 and M_2stop400 (**Supplementary Fig. 1**). The three in-frame methionines of the i3 loop, 248, 296 and 368, are highlighted in yellow; the translation of the C-terminal fragment starts from methionine 368. **b**, Schematic representation of the gene products that reach the plasma membrane of the wild type M_2, M_2trunk, M_2trunk and M_2tail and M_2stop228 (**Supplementary Fig. 1**). The M_2trunk and M_2tail genes generate the respective protein fragments that, only when co-transfected together, are able to form functional receptor complexes capable to bind ligands. The M_2stop228 gene mutant generates both M_2trunk (in green), when translation starts from the cap site, and M_2tail (in brown) when translation is cap-independent driven. This makes it likely that the truncated fragment of the M_2stop228 receptor may act as a chaperon driving part of the C-terminal-M_2 fragment to the plasma membrane, as supported by the binding and functional data shown by the co-transfection of M_2trunk(1-228) with M_2tail(368-466) (**Table 1**). **c**, Fluorescence micrographs of HEK293 cells respectively expressing M_2-EGFP, M_2stop228-EGFP, M_2fr.sh.-EGFP and M_2stop400-EGFP, together with an untransfected control. Imaging settings are the same for the five images, whereas contrast was adjusted to improve visualization. In the untransfected cells and stop400 panels, the contrast was set to 0. Insets display DIC image of the same field of view (scale bars 10 µm).

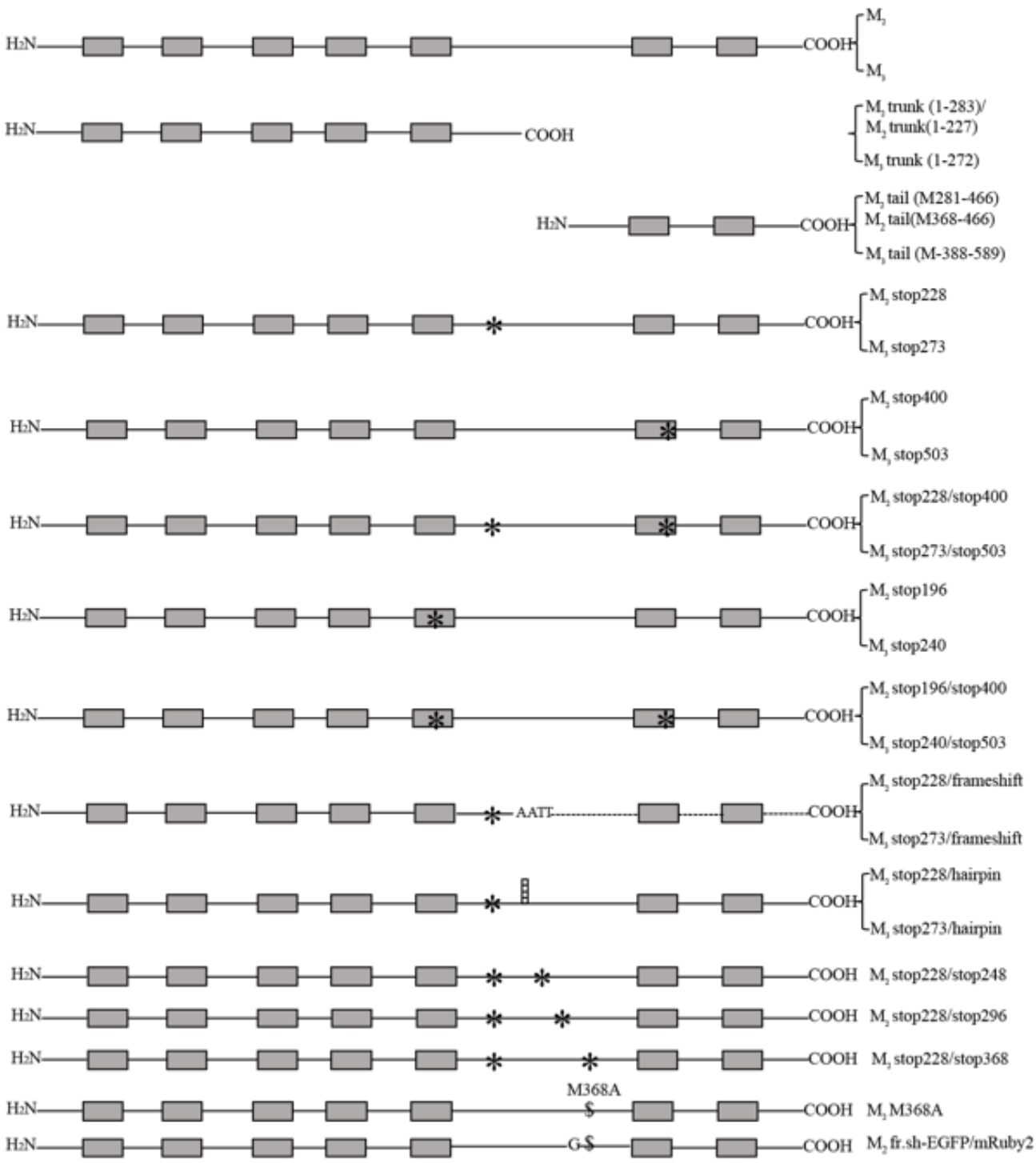

Supp. Fig. 1. Schematic representation of wild type muscarinic M_2 (human) and M_3 (rat) receptors and derived mutants. Each construct was obtained as described under "Materials and Methods". The asterisks represent the inserted stop codons while the $ symbol represents the substitution of methionine 368 with alanine, as in the M_2M368A construct, or the methionine 368 put out of frame after the insertion of a G nucleotide just before its codon, as in the M_2fr.sh.-EGFP construct. The hairpin loop in the M_2stop228/hairpin and M_3stop273/hairpin constructs, is indicated by a stacked column. With AATT is indicated the four nucleotides insertion that alters the reading frame of the M_2stop228/frameshift and M_3stop273/frameshift constructs.

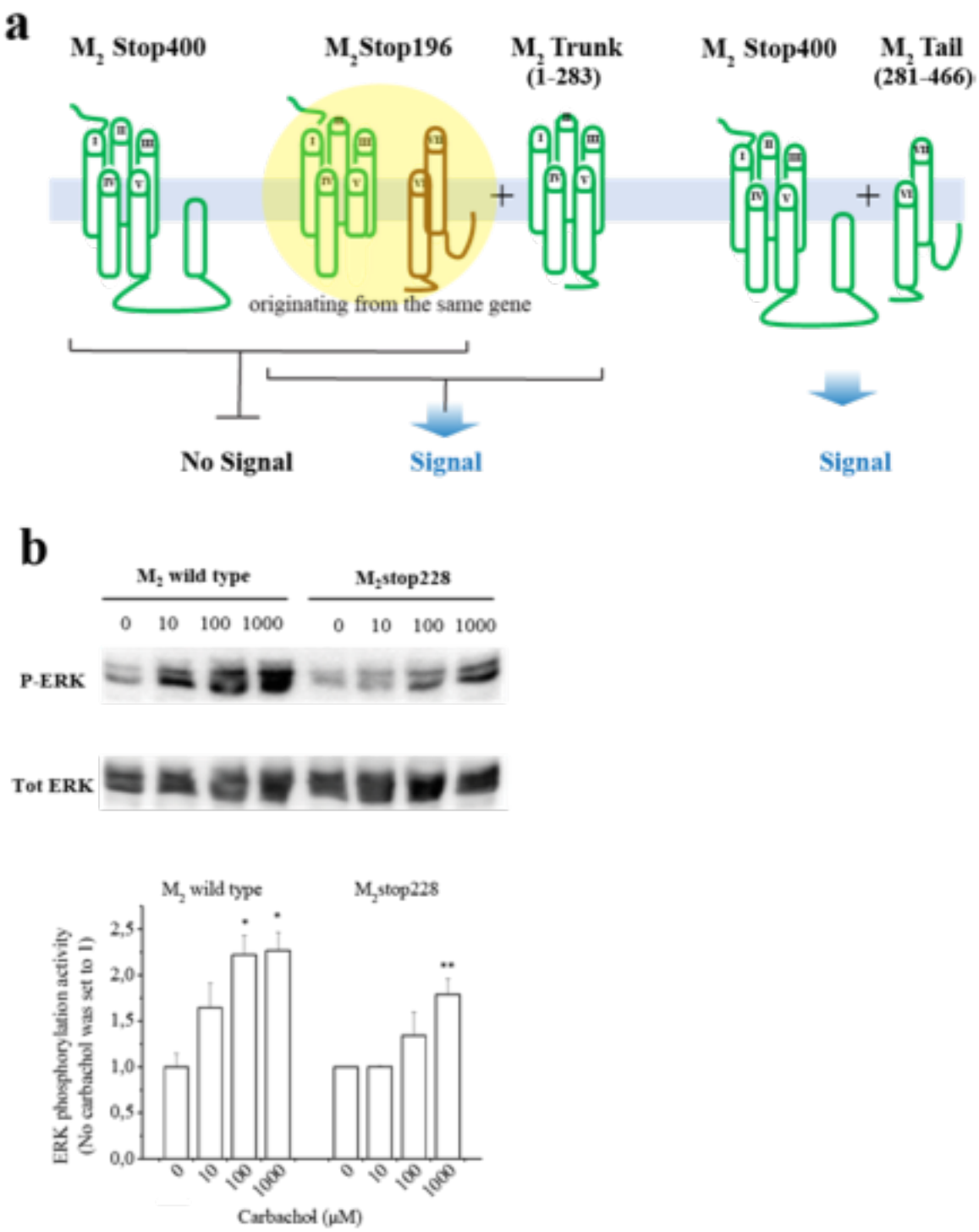

Supp. Fig. 2. M_2 receptor mutants with single and double stop codons. a, Schematic representation of the gene products M_2stop196 and M_2stop400, that are not functional by themselves but that are rescued by co-transfection with M_2Trunk(1-283) and M_2Tail(M-281-466), respectively. **b**, Dose response curve of carbachol induced ERK phosphorylation in HeLa cells transiently transfected with M_2 and M_2stop228 muscarinic receptors. Cells were stimulated for 5 minutes with the indicated concentration of carbachol. Phosphorylated ERK (P-ERK) was normalized vs total ERK (Tot ERK). Significance (*$p < 0.05$, **$p < 0.01$) was calculated against carbachol 0 μM.

Supplementary Table 1. Ligand binding and functional properties of M_2 receptor mutants with single and double stop codons. Number of [^{3}H]NMS binding sites for the indicated mutants. Untransfected COS-7 cells did not show any [^{3}H]NMS specific binding. N.B. = no specific [^{3}H]NMS binding.

Receptor	Bmax (fmol/mg)	Receptor	Bmax (fmol/mg)
M_2stop228	45.3 ± 2.4	M_2stop228/stop368	N.B.
M_2stop196	N.B.	M_2stop228/stop368 + M_2tail(281-466)	370± 20
M_2stop400	N.B.	M_2stop228/stop400	N.B.
M_2stop196+ M_2trunk(1-283)	47 ± 3	M_2stop228/stop400+ M_2tail(281-466)	380 ± 20
M_2stop400+ M_2tail(281-466)	400 ± 30	M_2stop196/stop400+ M_2trunk(1-283)	N.B.
M_2stop196/stop400	N.B.	M_2stop196/stop400+ M_2tail(281-466)	N.B.
M_2stop228/stop248	49 ± 5	M_2stop228/fr.sh.	47 ± 3
M_2stop228/stop296	38 ± 3	M_2stop228/Hairpin	37 ± 2

Supplementary Table 2. Radioligand binding and activation properties of M_3 receptor mutants. Binding characteristics and stimulation of phosphatidylinositol accumulation by M_3, M_3stop273 and the co-transfected M_3trunk(1-272) and M_3tail(M-388-586). Untransfected COS-7 cells did not show any [^{3}H]NMS specific binding. N.B. = no specific [^{3}H]NMS binding.

Binding data				Phosphatidylinositol accumulation assay	
Receptor	Bmax (fmol/mg)	[^{3}H]NMS KD (pM)	Carbachol IC50 (μM)	Carbachol EC50 (μM)	Maximum increase in IP_1 level above baseline (%)
M_3	1120 ± 71	29 ± 2	59 ± 4	4.2 ± 0.5	183 ± 15
M_3trunk(1-272)+ M_3tail(388-589)	114 ± 17	23 ± 2	48 ± 5	1.4 ± 0.1	126 ± 12

M_3stop 273	52.3 ± 0.5	31.3 ± 2.8	56 ± 2	1.1 ± 0.1	89 ± 13

Supp. Table 3. Ligand binding of M_3 receptor mutants with single and double stop codons. Number of [^{3}H]NMS binding sites in COS-7 cells transiently transfected with the indicated M_3 receptor mutants with single and double stop codons.

Receptor	Bmax (fmol/mg)	Receptor	Bmax (fmol/mg)
M_3stop273	54 ± 1	M_3stop273/stop503	N.B.
M_3stop240	N.B.	M_3stop273/stop503 + M_3tail(388-589)	120± 15
M_3stop503	N.B.	M_3stop240/stop503+ M_3trunk(1-272)	N.B.
M_3stop240+ M_3trunk(1-272)	44 ± 3	M_3stop240/stop503+ M_3tail(388-589)	N.B.
M_3stop503+ M_3tail(388-589)	135 ± 12	M_3stop273/fr.sh.	120 ± 4
M_3stop240/stop503	N.B.	M_3stop273/Hairpin	30 ± 2

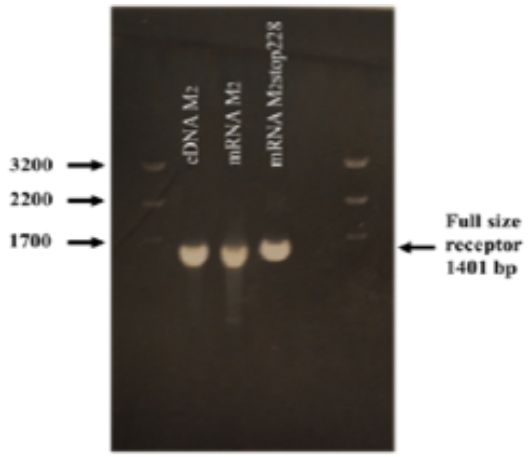

Supp. Fig. 3. Lack of alternative splicing in M_2 wild type and M_2stop228 receptors. mRNAs were extracted by COS-7 cells transfected with M_2 wild type and M_2stop228, subjected to reverse transcriptase and the resulting cDNA amplified by PCR with two oligos directed to the 5' and 3' end of the receptors. The gel shows, in both M_2 wild type and M_2stpo228,

a single band of 1401 bp corresponding to the full-size receptor, running at the same level of the band amplified directly form the M_2 pcD plasmid.

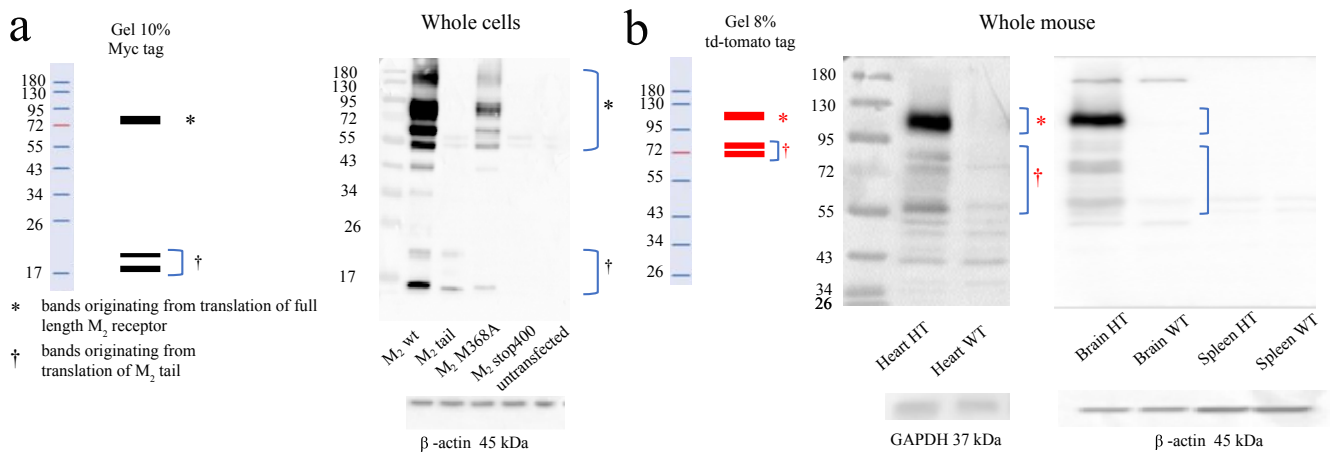

Fig. 2. Western blot of tagged M_2 receptor mutants in HEK293 cells and in tdtomato knock-in mice. a, left Graphical guide of the fragments observed on the gel when using myc-tag. **right**, M_2-myc, M_2tail(368-466)-myc, M_2M368A-myc and M_2stop400-myc were transiently transfected in HEK293 cells and immunodetected via antimyc primary antibody, together with an untransfected control. Loading control normalization was performed vs β-actin **b**, **left** Graphical guide of the fragments observed on the gels when using the tdtomato tag. **right**, Western blot from tissue preparations originating from the indicated organs of M_2-tdtomato knock-in mice (HT) and wild-type animals (WT). Immunodetection was performed using an anti-tdtomato primary antibody. Loading control normalization was performed using GAPDH in the heart, and β-actin in the brain and spleen.

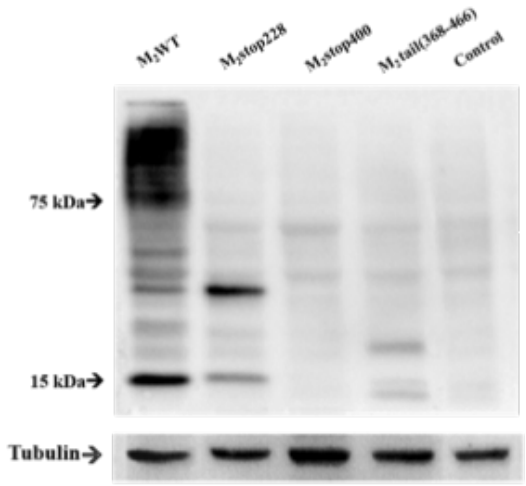

Supp. Fig. 4. Western blot of tagged M_2 receptor mutants in COS-7 cells. a, M_2-myc, M_2stop228-myc, M_2stop400-myc and M_2tail(368-466)-myc containing the human myc tag at C-terminal were transiently transfected in COS-7 cells and immunodetected via Western blot after SDS-Triton protein extraction. Both M_2 wild type, M_2stop228 and M_2tail(368-466 showed 15 kDa bands corresponding to the C-terminal fragment. The 75 kDa bands indicated by the arrows in M_2 WT corresponds to the full lenght wild type M_2 receptor. On the contrary, M_2stop400 did not show any band, similar to the control.

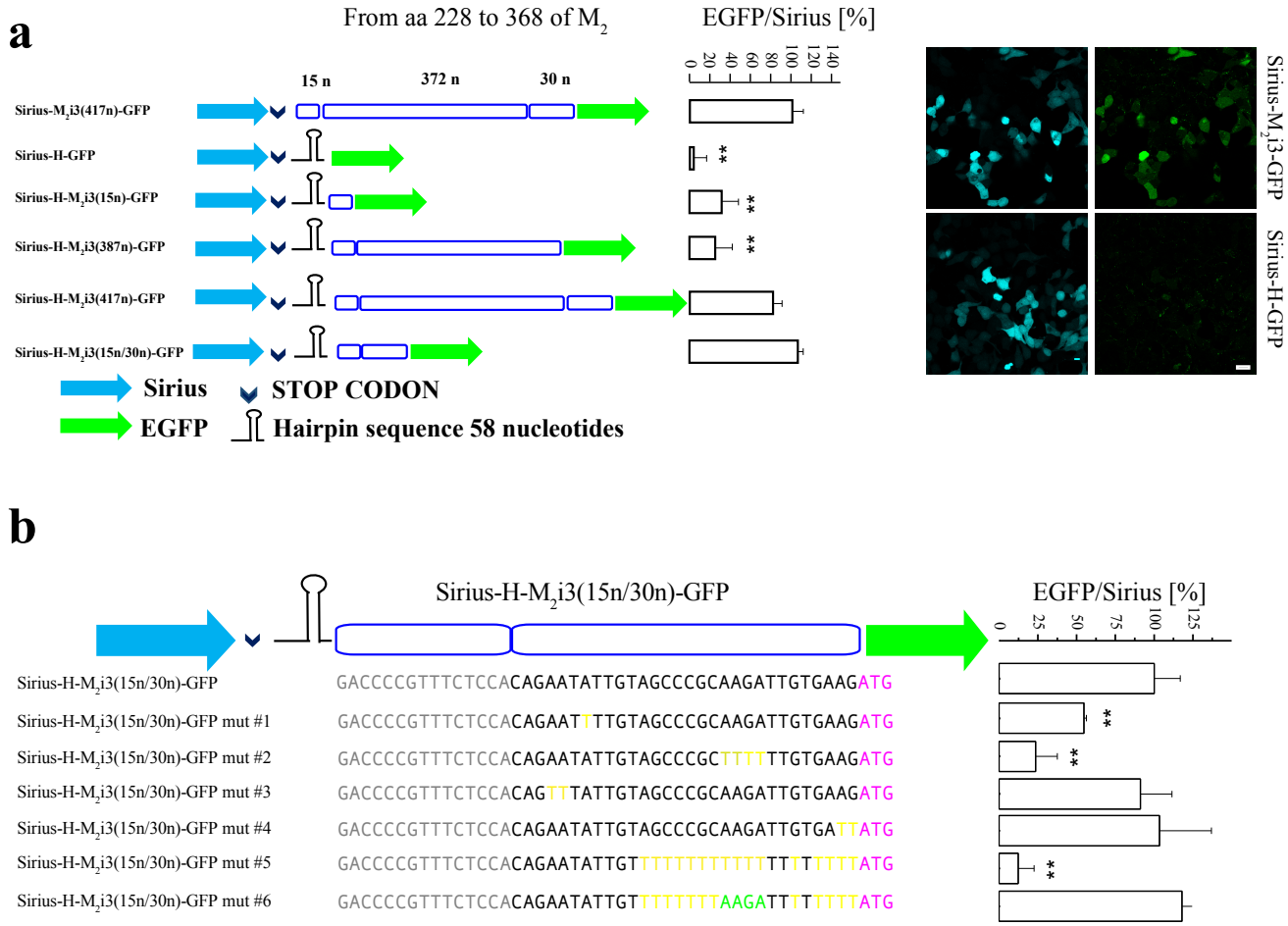

Fig. 3. Fluorescence assay of cap-independent translation of EGFP driven by the i3 loop mutants of the muscarinic M_2 receptor. a, **left** Schematic representation of bicistronic plasmids bearing the M_2 i3 loop between the coding regions of the Sirius and EGFP fluorescent proteins. A guanine nucleotide was originally inserted before the EGFP in the plasmid Sirius-H-EGFP in order to maintain in frame the sequences of the two fluorescent proteins. In all the other plasmids the sequence of the two fluorescent proteins is not in frame. Fifteen nucleotides derived from the M_2 i3 loop were inserted between the end of Sirius and the hairpin loop, in order to allow the easy scanning of the ribosome across the stop codon. **right**, Relative fluorescence of EGFP compared to Sirius, highlighting the efficiency of cap-independent translation for the control Sirius-M_3i3(417n)-EGFP and the six mutants. The insert shows the difference in the green fluorescence between two of the mutants. **b**, **left** Mutations of the bicistronic Sirius-H-M_2i3(15n/30n)-EGFP plasmids in the region of the M_2 i3 loop from nucleotides 1972 to 2001, in yellow are the modified nucleotides. In Sirius-H-M_2i3(15n/30n)mut#6-EGFP the four nucleotides in green (AAGA) were reinserted in the stretch of 20 T of Sirius-H-M_2i3(15n/30n)mut#5-EGFP. **right** Relative fluorescence of EGFP compared to Sirius, highlighting the efficiency of cap-independent translation for the control Sirius-H-M_2i3(15n/30n)-EGFP and the six mutants illustrated. Significance ($p < 0.01$) was calculated in **a** against Sirius-M_2i3(417n)-EGFP and in **b** against Sirius-H- M_2i3(15n/30n)-EGFP. Error bars are s.e.m.

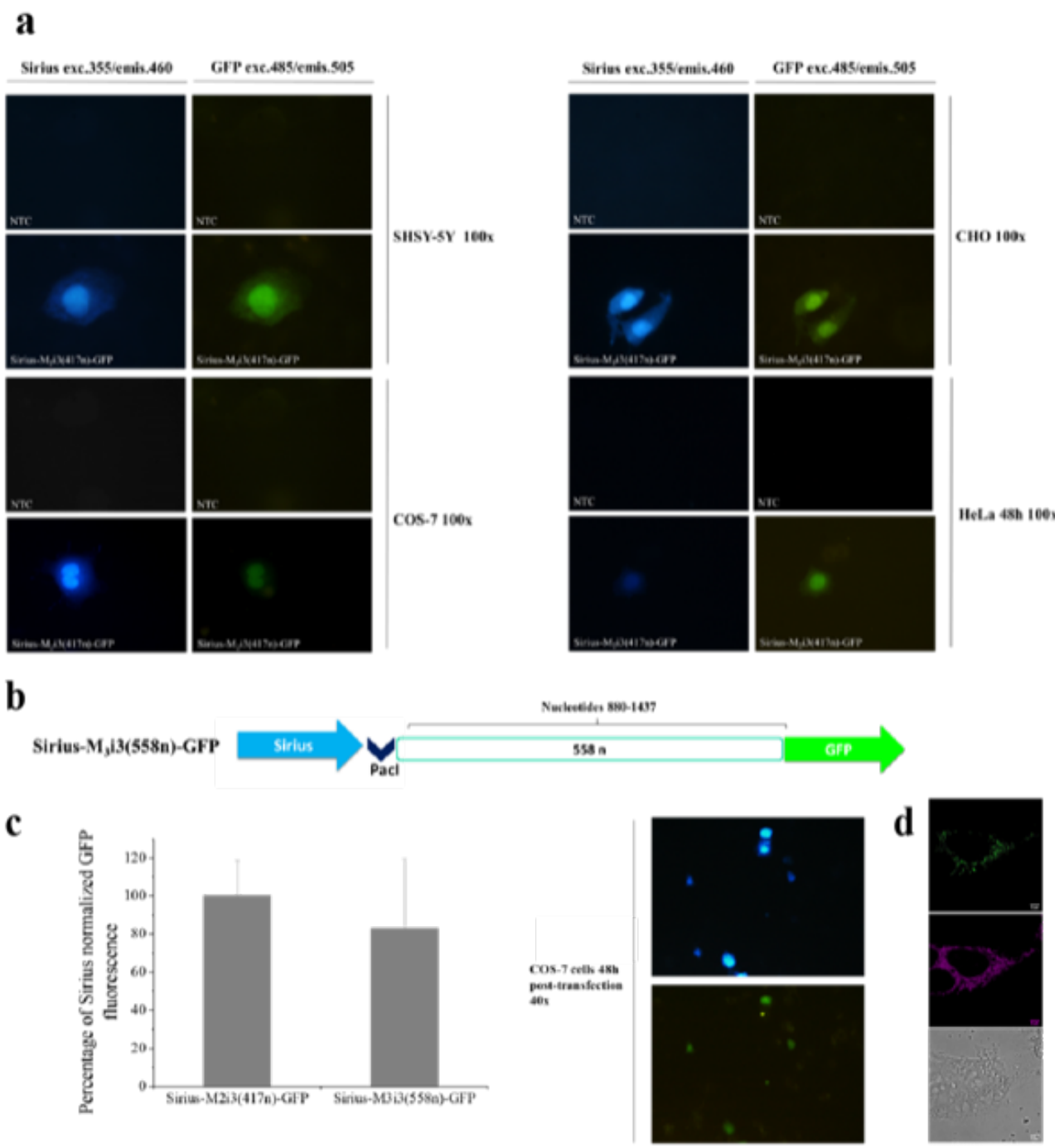

Supp. Fig. 5. Expression of the bicistronic plasmid Sirius-M_2i3(417n)-EGFP in four different cell lines and of the bicistronic plasmid Sirius-M_3i3(558n)-EGFP in COS-7 cells. a, Expression of Sirius was driven by the canonical scanning mechanism of translation initiation, while EGFP expression was driven by an IRES dependent mechanism. All Sirius-M_2i3(417n)-EGFP transfected cells expressed both the Sirius and EGFP proteins. On average, 25 ± 4% of the COS-7 cells transfected with Sirius-M_2i3(417n)-EGFP plasmid were blue fluorescence positive, while 17 ± 2% were green fluorescent positive, with only a few cells being only green. **b**, Schematic representation of the bicistronic plasmid bearing the i3 loop of the rat muscarinic M_3 receptor (558 nucleotides from nucleotide 880 to nucleotide 1437) between the coding regions of the Sirius and EGFP fluorescent proteins. **c**, EGFP expression in COS-7 cells transfected with the bicistronic plasmid Sirius-M_3i3(558n)-EGFP. **d,** (top) Confocal images of M_2-Hairpin-EGFP, (middle) Mitotracker staining, (bottom) DIC. Scale bars 10 µm.

```
         1072                                1104
         ↓                                   ↓
CHRM2    CAGAATATTGTAGCCCGCAAGATTGTGAAGATG          ATG (Met368 in the i3 loop) is 57 nucleotides from TMD6
CHRM4    GCTCGCAACCAGGTGCGCAAGAAGCGGCAGATG          ATG (Met391 in the i3 loop) is 30 nucleotides from TMD6
CHRM1    GAGAGGAGCCTGGCTCCGAAGTGGTGATCAAGATG        ATG (Met304 in the i3 loop) is 186 nucleotides from TMD6
CHRM3    ACCAGAAGTCAGATCACTAAGCGGAAAAGGATG          ATG (Met481 in the i3 loop) is 30 nucleotides from TMD6
CHRM5    ACCAACAATGGCTGTCACAAGGTGAAAATCATG          ATG (Met403 in the i3 loop) is 120 nucleotides from TMD6
```

Supp. Fig. 6. Alignment of the nucleotide sequence 1072-1104 of the M_2 i3 loop with analogous sequences of the other four muscarinic receptors. The criteria for the alignment are described in the supplementary data. In yellow are highlighted the conserved nucleotides. In bold are the in frame ATG codons. Next to each sequence is indicated the codon number of the in-frame ATG and its distance in nucleotides from the beginning of TMDVI.

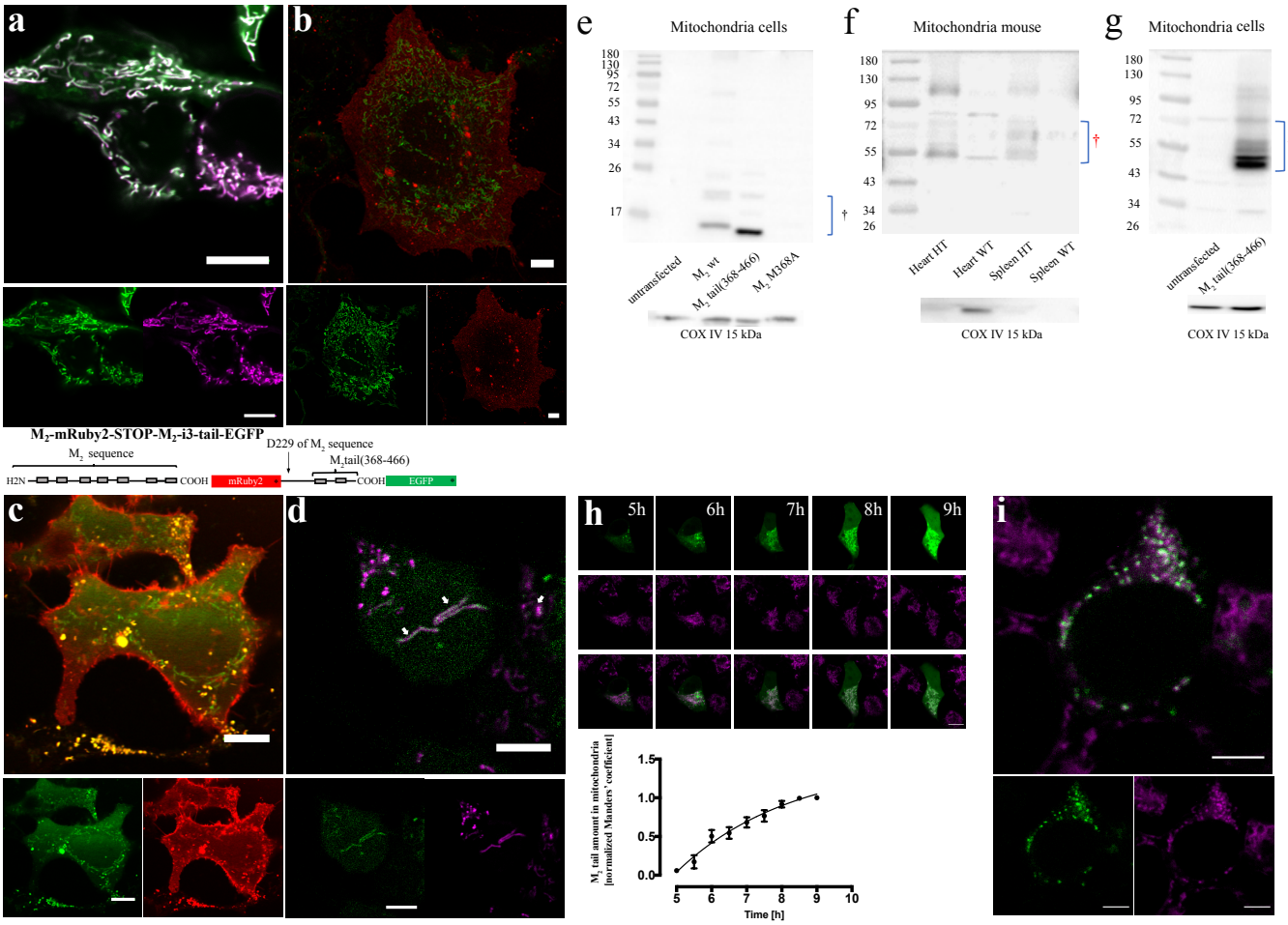

Fig. 4. Localization of fluorescently labeled M_2 mutant constructs: microscopy and western blots analysis. a, Colocalization of M_2tail(368-466)-EGFP (green) together with the mitochondrial targeted dye Mitotracker (magenta) in HEK293 cells. Separate spectral channels are displayed below. **b**, Co-expression of M_2tail(368-466)-EGFP (green) and wild type M_2-mRuby2 (red) in HEK293 cells. Separate spectral channels are displayed below. **c**, Cellular localization of the construct M_2-mRuby2-STOP-M_2-i3-tail-EGFP in HEK293 cells. Expression of the M_2tail(368-466)-EGFP (green) after the STOP codon is an indicator of the endogenous IRES activity. While M_2-mRuby2 localizes correctly and predominantly to the cell plasma membrane, M_2tail(368-466)-EGFP localizes in the cytosol as well as, strongly, to the cell mitochondria. Separate spectral channels are displayed below. **d**, M_2-fr.sh.-EGFP (green) expressed in conjunction with Mitotracker (magenta). The EGFP is expressed despite the creation of an in-frame stop after M368, confirming endogenous cap-independent translation of the M_2tail(368-466). Arrows indicate areas of colocalization with the mitochondria. Separate spectral channels are displayed below. **e**, Western blot (10% TRIS-Glycine PAA gel) of mitochondria purified from Hek293 cells transfected with the M_2-Myc, M_2tail(368-466)-Myc, M_2M368A-Myc, together with an untransfected control are blotted using an anti-myc antibody. Loading control was verified by immunoblotting COXIV. **f**, Western blot (8% TRIS-Glycine PAA gel) of mitochondria purified from tissue preparations originating from the indicated organs of M_2-tdtomato knock-in mice (HT) and wild-type animals (WT), detected using an anti-tdtomato antibody. Please note that the band at 80kDa is aspecific, and is more prominent in the WT lane due to higher loading. **g**, Western blot (8% TRIS-Glycine PAA gel) of mitochondria purified from HEK293 cells transfected with the M_2tail(368-466)-tdtomato, together with an untransfected control. Mitochondrial proteins were blotted using an anti-tdtomato antibody. Loading control was verified by detecting the 15 kDa mitochondrial matrix protein Cox-IV. **h** Time course of

M_2tail(368-466)-EGFP import in the mitochondria of a HEK293 cell over a 4h interval, starting 5h after cell transfection, as indicated. Panels, from top to bottom show M_2tail(368-466)-EGFP (green), Mitotracker (magenta) and overlay displaying increasing colocalization over time. Chart at the bottom quantifies colocalization of the M_2tail(368-466)-EGFP in the mitochondria by calculating the Manders Coefficients (n=7 cells, from 3 independent transfections, error bars are s.e.m.) (See **Methods**). **i**, Detail of a HEK293 cell expressing the M_2-GFP11 construct together with pmito-GFP1-10. The M_2-GFP11 was sequentially transfected 24 h after the pmito-GFP1-10 (see **Methods**) Magenta overlay indicates mitotracker. White signal in the overlay indicates M_2tail(368-466) trafficking to the organelle. All confocal micrographs were obtained by sequential imaging using 488 nm excitation and detection in the 520-600 nm (EGFP), 561 nm excitation and detection in the 580-650 nm (mRuby2) and at 633 nm and detected in the 650-700 nm range (Mitotracker) using HyD detectors in Photon Counting Mode. Scale bars are 10 µm throughout.

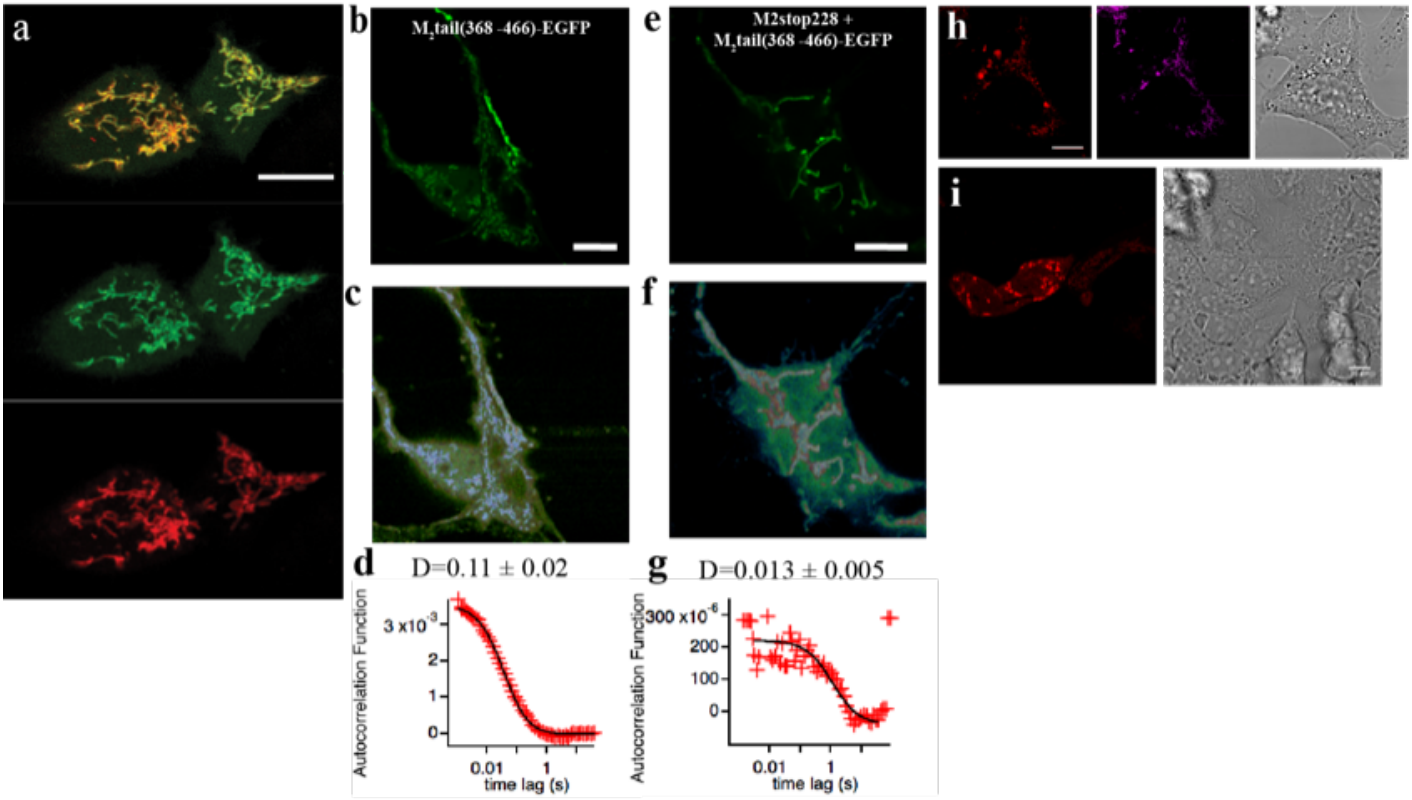

Supp. Fig. 7. Subcellular localization of the M2tail(368-466). a, Confocal image displaying the colocalization (top) of M2tail(368-466)-EGFP (green, middle)) in HEK293 cells, co-expressed with the outer mitochondrial membrane marker Tom20-mCherry (red, bottom). **b** expression of M2tail-EGFP displaying marked mitochondria and cytosolic localization. **c**, Glasbey colorscale representation of panel (**b**) highlighting the low-intensity pixels. **d**, autocorrelation function of the M_2tail(368-466)-EGFP diffusion taken at or in proximity of the basal membrane, yielding a mean diffusion coefficient of 0.11 $\mu m^2/s$, incompatible with membrane diffusion. **e**, co-expression of M_2stop228 and M_2tail(368-466)-EGFP. M_2stop228 is unlabeled. M_2tail(368-466)-EGFP maintains the localization to the mitochondria observed in cells expressing M_2tail(368-466)-EGFP alone, but it is also localized to the plasma membrane, visible in panel **f**, Glasbey colorscale representation of panel **e** highlighting the low-intensity pixels. **g**, autocorrelation function of the M_2tail(368-466)-EGFP diffusion taken at or in proximity of the basal membrane, yielding a mean diffusion coefficient of 0.013 $\mu m^2/s$, compatible with membrane diffusion. **h**, Cellular localization of M_2tail-mRuby2, together with Mitotracker deep

red staining of the mitochondrial network and corresponding DIC image. **i,** Cellular localization of M_2tail-tdtomato and corresponding DIC image. All panels originate from Laser Scanning Confocal Microscope sequential acquisitions, with laser lines 488 nm (EGFP) 561 nm (mRuby2 and tdtomato) and 633 nm (Mitotracker deep red), and corresponding emission filters in the ranges 520-600 nm, 570-620 nm and 640-750 nm. Scale bars 10 µm.

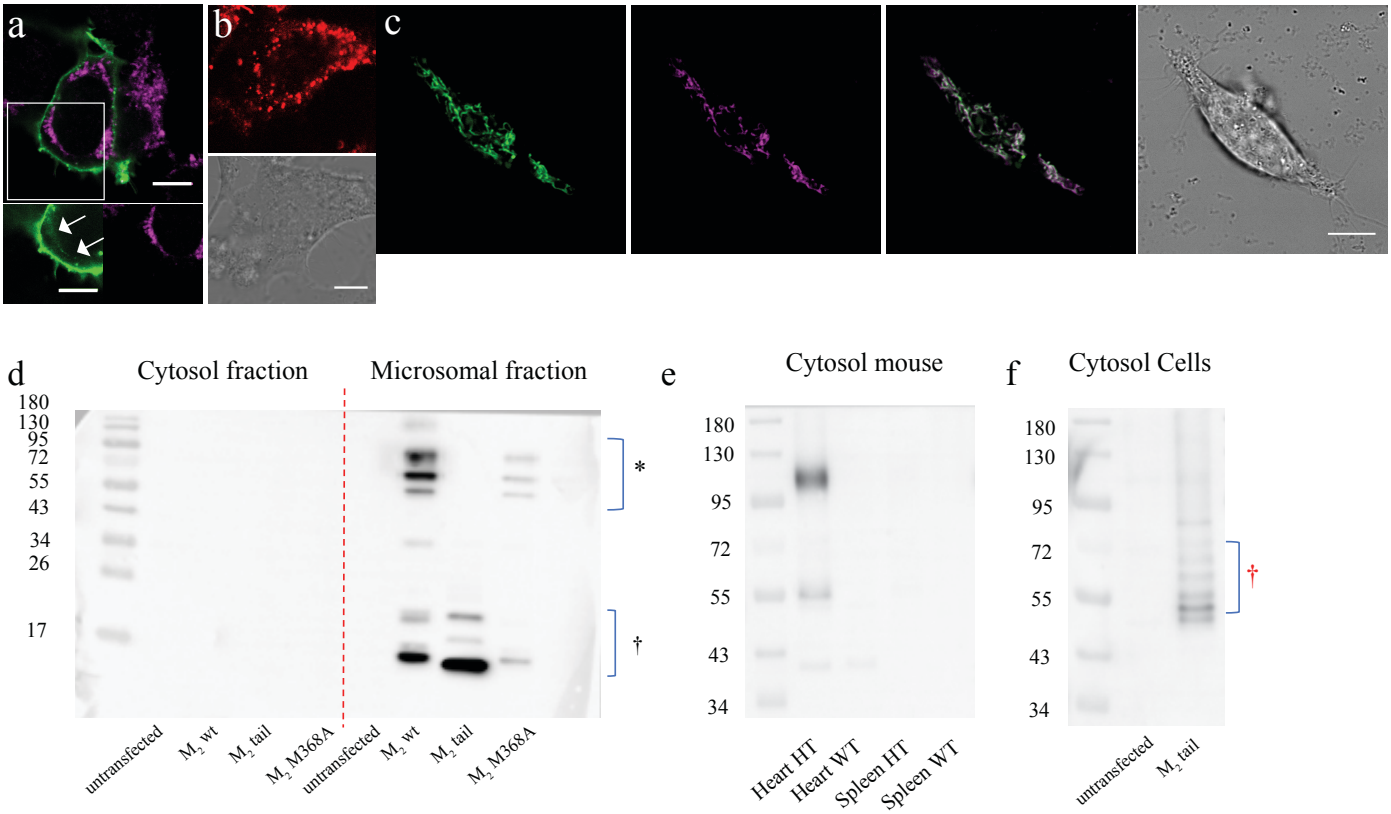

Supp. Fig. 8. **Mitochondrial localization of the M2tail fragment**. **a**, Confocal image of M_2-EGFP (green) expressed in conjunction with Mitotracker (magenta) in HEK293 cells. Separate panels below. **b,** Confocal image of HEK293 cell expressing *M_2fr.sh-mRuby2*, together with DIC, below. **c**, Confocal sequential images displaying the localization of fluorescently labeled M_2tail(368-466)-EGFP (green), together with the mitochondrial network (magenta), colocalization (white) and DIC image in COS-7 cells. Scale bars are 10 µm. Confocal sequential acquisitions were performed with 488 nm excitation and 520-600 nm detection (EGFP), and with 561nm excitation and 600-750 nm detection (mCherry) and 633 nm excitation and 650-750 nm detection (Mitotracker) using HyD detectors in Photon Counting Mode. **d,** Western blot (10% TRIS-Glycine PAA gel) of the cytosolic and microsomal fractions resulting from the mitochondria purification of lysates of HEK293 transfected with myc-tagged constructs, as displayed in **Fig. 4e**. **e**, Western blot (8% TRIS-Glycine PAA gel) of the cytosolic fraction resulting from the mitochondria purification of lysates of HT and WT tissues of a tdtomato transgene mice, as displayed in **Fig. 4f.** **f**, Western blot (10% TRIS-Glycine PAA gel) of the cytosolic fraction resulting from the mitochondria purification of lysates of HEK293 transfected with M_2tail(368-466)-tdtomato, as displayed in **Fig. 4g**.

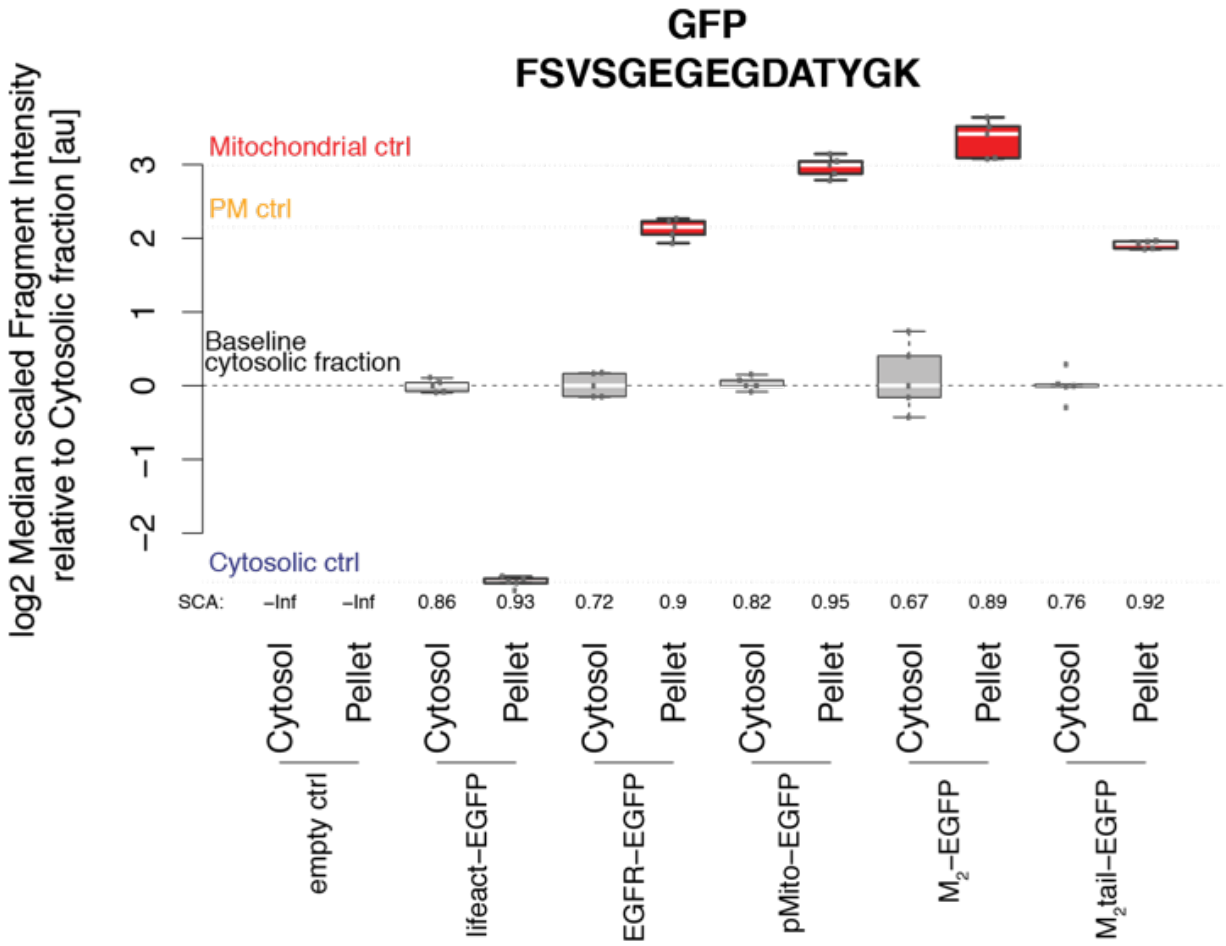

Supp. Fig. 9 Relative abundance estimates of EGFP and M_2 receptor from PRM based mass spectrometric measurements. Normalized fragment intensities were calculated for the peptide FSVSGEGEGDATYGK (specific for EGFP) for cytosolic and pellet fractions and for different constructs. Each preparation was normalized relative to the cytosolic fraction, if data was available. Median levels of cytosolic, plasma membrane and mitochondrial control markers are shown in the left panel. For each identified peptide the normalized spectrum contrast angle, indicating the similarity of the recorded spectrum to the reference spectrum, is indicated below each plot.

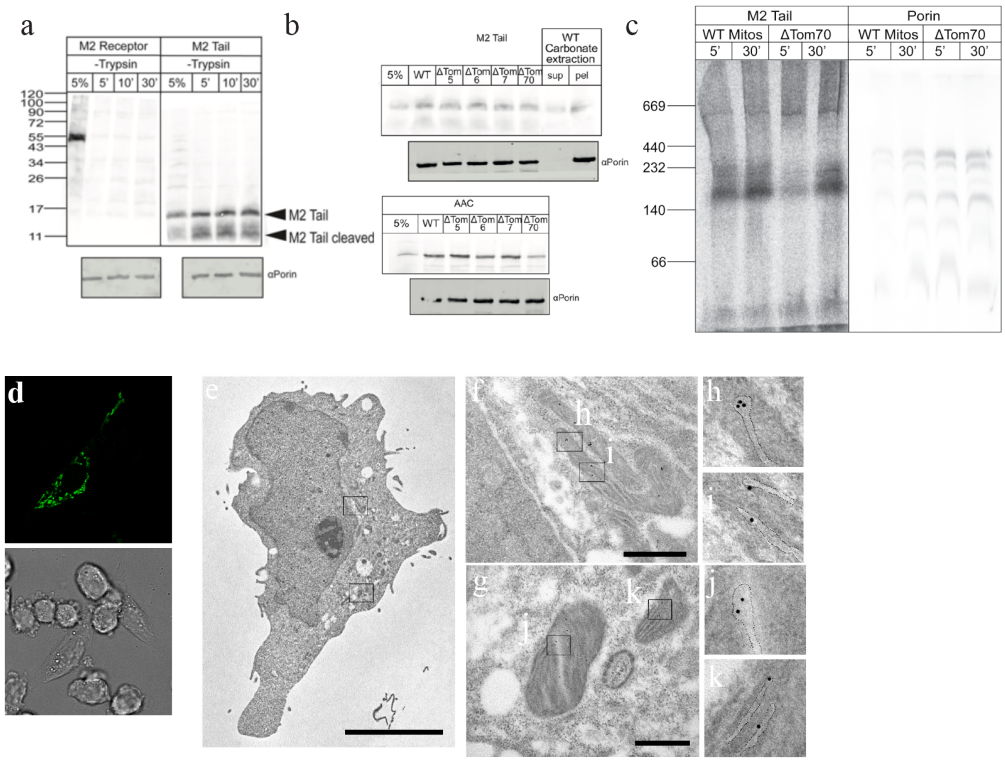

Supp. Fig. 10. In vitro mitochondrial import of M_2tail(368-466) and electron microscopy of M_2stop228. a, Import of M2-tail fragment in yeast mitochondria: 35S-labelled and translated in-vitro full length muscarinic M_2 receptor or M_2tail(368-466) expressing 5 C-terminal Methionines were incubated with isolated yeast mitochondria for various timepoints in the presence of the inner membrane potential (**See Supplementary Methods**). Samples were then washed in breaking buffer and loaded onto a 12% Tris-Tricine gel followed by semi-dry transfer and visualized via a phosphorimager. 5% of the crude protein was loaded as a control (left lane). To test for equal mitochondrial loading, αPorin was probed via western blot. The kinetics pattern of M_2tail is what it is expected for a protein imported in mitochondria: the appearance of the cleaved M_2-tail is indicative of a processing of the fragment once imported in mitochondria. **b,** ^{35}S-labelled M_2tail(368-466) or AAC (an integral internal mitochondrial membrane protein) were imported into isolated yeast mitochondria originating from different knock-out lines for outer membrane transporters (ΔTom). Samples were incubated for 30 minutes, and then washed in breaking buffer. After import, 100 µg of mitochondria were subject to Carbonate extraction to determine if M_2tail(368-466) is integrated into a lipid bilayer (Pellet) or loosely associated/soluble (Supernatant). Samples were then loaded onto a 12% Tris-Tricine gel followed by semi-dry transfer and visualized via a phosphorimager. To test for equal mitochondrial loading anti-αPorin was used via western blot. **c,** ^{35}S-labelled M_2tail(368-466) and αPorin were imported into isolated wild-type or ΔTom70 mitochondria for the indicated timepoints. Samples were then washed in breaking buffer and loaded on blue-native page followed by gel drying and visualized via a phosphorimager. **d,** Confocal images displaying the mitochondrial localization of M_2tail-GFP11 + M_2tail-GFP1-10, with corresponding DIC image. **e**, TEM micrograph of a COS-7 cell showing a large nucleus, several mitochondria and vacuoles nearby. Bar: 5 µm. **f-g**, High magnification of portion of the cell cytoplasm showing a few gold particles confined to the mitochondria. Bar: 500 nm. **h-k,** Gold particles appear associated with the mitochondrial cristae, highlighted by the dotted line. A total number of 236 gold particles in 40 mitochondria from 19 sections were detected.

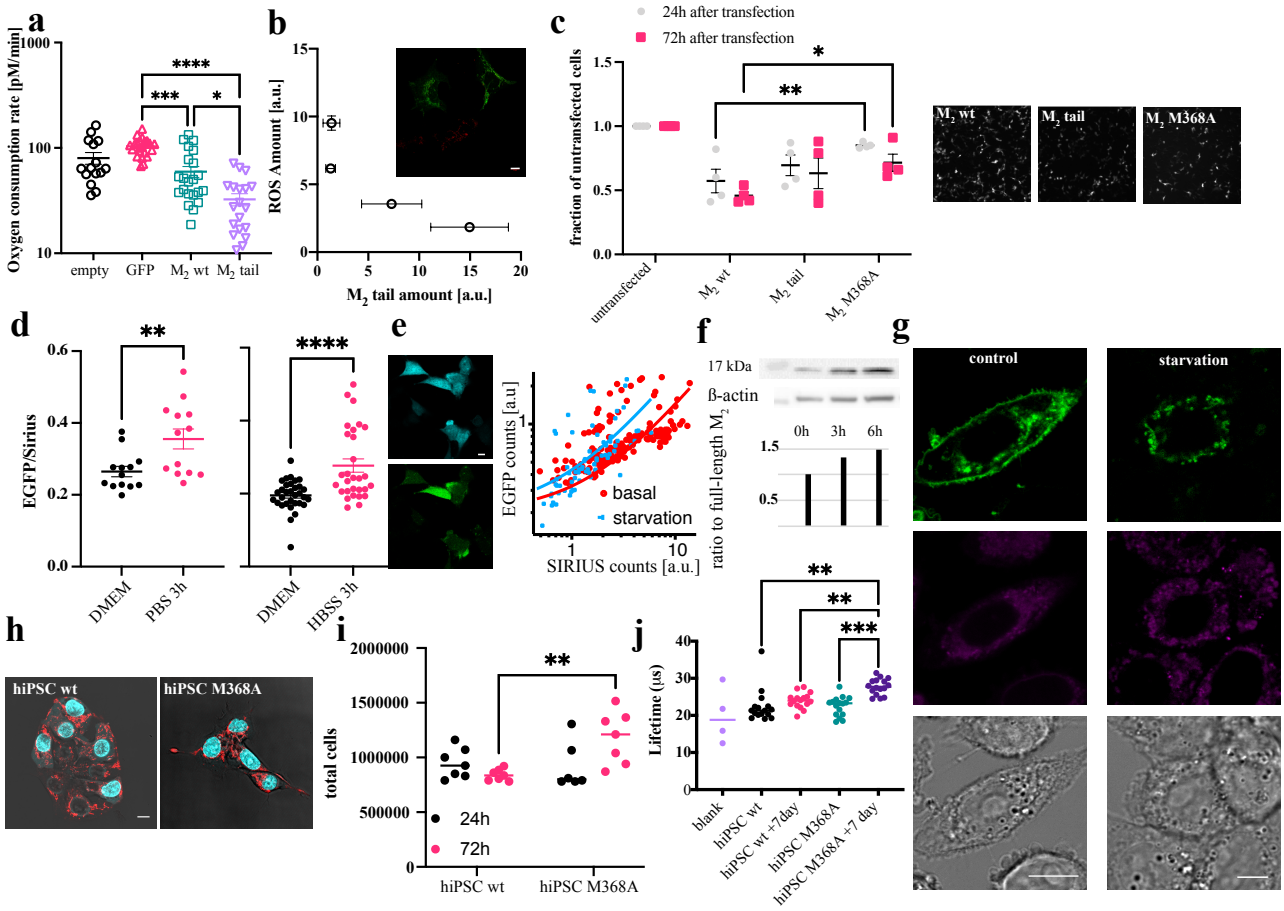

Fig. 5. Effects of M_2 mutants on mitochondrial function and cell metabolism. a, Basal oxygen consumption upon HEK293 cell stress -following starvation- measured by a Seahorse assay at a constant temperature of 37 °C. **b**, Localization of M_2tail(368-466)-EGFP in HEK293 (green) cells stained with a marker for reactive oxygen species (Cell Rox Deep Red, ThermoFisher). Relationship between green (M_2tail abundance) vs red (amount of ROS produced) fluorescence intensities measured from regions of the mitochondrial network. The data were binned in four groups as a function of the amplitude of Cell Rox Deep Red signal (0-2.5, 2.5-5. 5-7.5 and 7.5-10 intensity counts). **c**, Cell viability assay performed on HEK293 cells transfected with M_2, M_2tail(368-466) and M_2(M368A), compared to an untransfected control. Cells were counted 24h and 72h after transfection in T-25 flasks, exposed throughout to 100 nM atropine. The experiments were performed in two biological replicates, each with two technical replicates. Transfection efficiency (to the right of the chart) was monitored thanks to the mRuby2 fluorescent reporter within a bicistronic cassette within each vector (see Methods). **d**, 96-well plate reader measurement of the increase of EGFP fluorescence relative to Sirius in COS-7 cells transfected with the bicistronic Sirius-M_2i3(417n)-EGFP plasmid and starved for three hours respectively in PBS (left panel) (n= 3 transfections, 16 wells) and HBSS (right panel) (n=1 transfection, 16 wells). **e,** Representative single cell confocal and DIC micrographs of HEK293 cells expressing the Sirius-M_2i3(417n)-EGFP construct in basal conditions, together with scatter plot of the average EGFP and Sirius fluorescence intensity values measured from single cells in basal (red dots) and 3h HBSS starvation (blue dots) conditions. **f**, Western blot from whole cell lysates of HEK293 cells transfected with the M_2-myc receptor, subject to increasing levels of serum starvation, as indicated. Shown is the M_2tail(368-466) band. The corresponding chart displays the intensity ratio of the M_2tail(368-466) band to the full length M_2 band (not displayed here)**.** Loading control was performed by using **β**-actin. **g**, HEK293 cells were sequentially transfected with pMito-GFP1-10 (24h) and M_2-GFP11 (8h, of which 6h under starvation conditions). (left panels) HEK293 cells grown in full culture medium and (right panels) HEK293 cells starved for 6 h after transfection of M_2-

GFP11.Shown are EGFP fluorescence (top), Mitotracker (center) and DIC (bottom). **h**, Confocal micrographs of wt hiPSCs (left) and those harboring the M368A mutation within the M_2 gene (right), stained with DAPI (cyan) and Mitotracker (red). **i**, Cell proliferation assay performed for wt hiPSCs and M368A hiPSCs grown in T25 flasks. Cells were counted 24h and 72h after seeding. **j**, Extracellular oxygen consumption assay, performed on wt and M368A hiPSCs, prior to and after 7 days undirected differentiation. The lifetime of a commercial dye increases as oxygen in the medium is progressively consumed by the cells. The data displayed are collected after 60 minutes incubation.

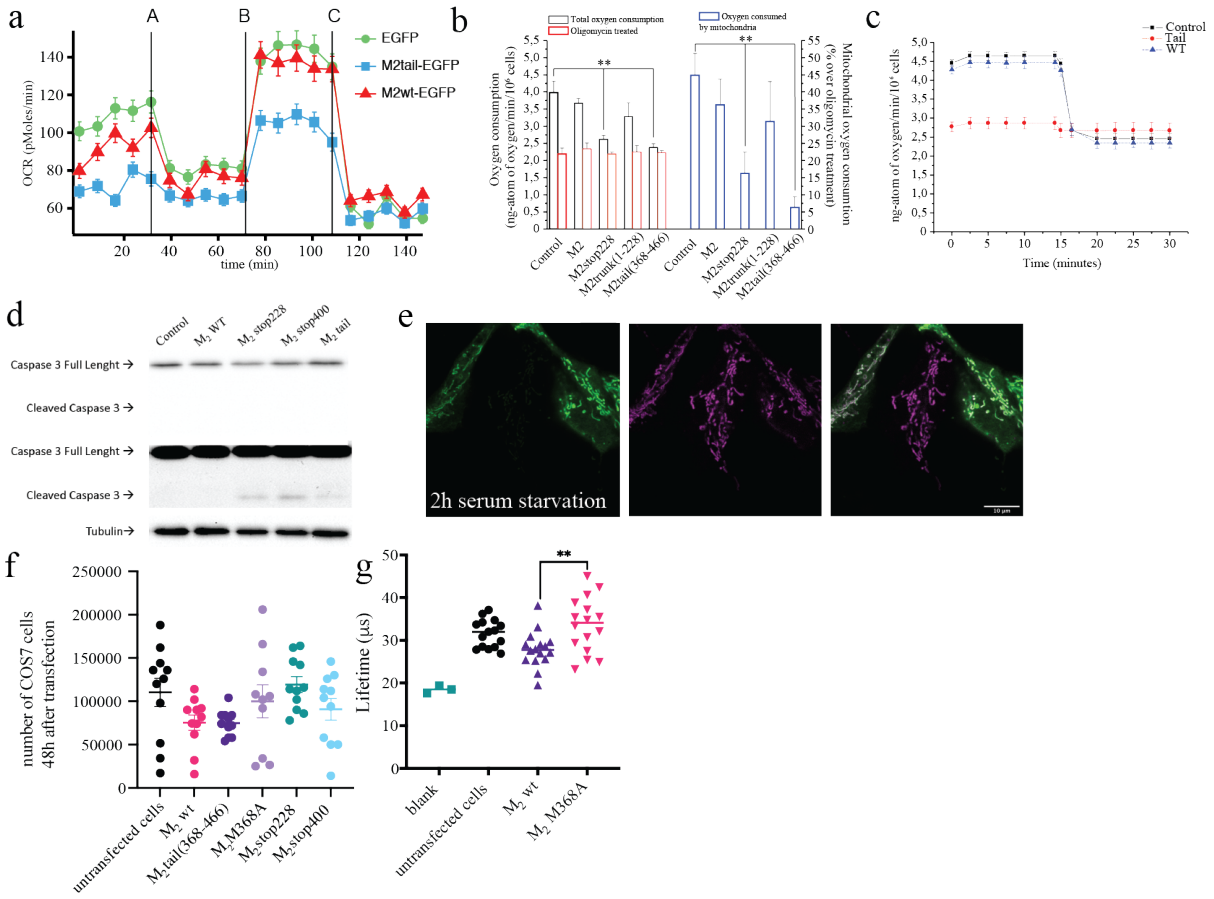

Supp. Fig. 11. Supplemental data on the effect of the M_2tail(368-466) fragment on mitochondrial function and cell metabolism. a, Representative experiment of Seahorse assay showing the time course of oxygen consumption inhibition by M_2tail(368-466)-EGFP and wild type M_2-EGFP, compared to the same experiments performed in control cells transfected with EGFP. The rate of ATP-linked respiration measured after oligomycin administration is decreased in M_2tail and slightly decreased in M_2 cells as well as compared to the controls. FCCP, an ionophore, was added to each cell type to investigate the cellular bioenergetic reserves that seem to be slightly reduced only in the M_2 tail cells. **b**, Oxygen consumption measured by a Clark type electrode-based-polarographic method at a constant temperature of 37 °C. After 15 minutes of basal respiration, the ATP synthase inhibitor oligomycin was added at a concentration of 17 nM. Oxygen consumption in the absence and presence of oligomycin is represented by black and red bars, respectively. The blue bars represent the percentage of mitochondrial oxygen consumption (total minus oligomycin treated) in cells transfected with each construct. **c**, is a representative experiment showing the time course of inhibition of oxygen consumption by M_2tail(368-466), compared to the same experiments performed in control cells and cells transfected with the M_2 wild type construct, upon addition of oligomycin. Results are given as ng-atom of oxygen/min/10^6 cells. **d**, Western blot of caspase-3 cleavage in COS-7 cells transfected with the indicated M_2 receptor mutants 48h after transfection (top panel, normal

contrast; bottom panel, increased contrast). **e,** Confocal sequential images of M_2tail(368-466)-EGFP (green), Mitotracker (magenta) and overlay upon 2h of serum starvation. Scale Bars are 10 µm. **f**, Cell viability assay performed in COS-7 cells 48 hours after transfection with M_2, M_2stop400, M_2tail(368-466), and M_2(M368A), compared to control untransfected cells. Data derive from n=4 independent transfections. **g,** Extracellular oxygen consumption assay of HEK293 cells transfected with the indicated M_2 receptor mutants using a fluorogenic dye quenched by Oxygen. Blank indicates the dye lifetime measured in wells containing the dye, but no cells.

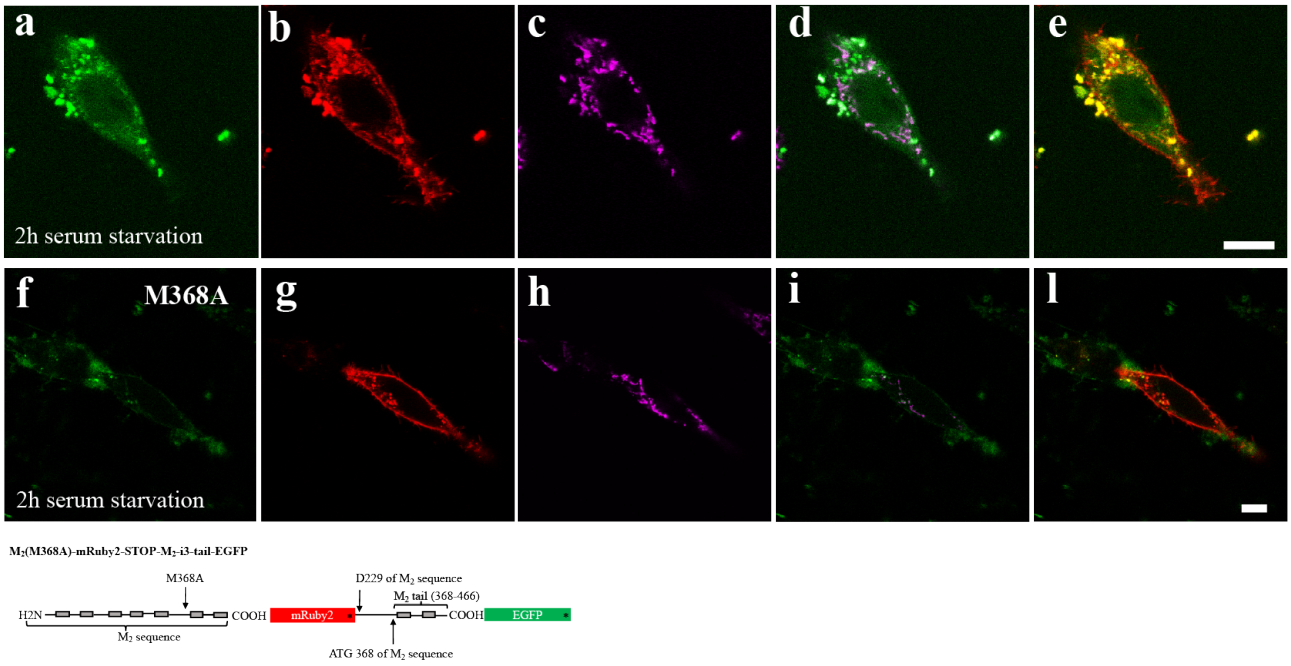

Supp. Fig. 12. Functional aspects of mitochondrial localization of the M_2tail(368-466) fragment. a-e, Mitochondrial localization of the IRES mediated C-terminal fragment is enhanced upon cellular stress. HEK293 cells transfected with the super construct M_2-mRuby2-STOP-M_2-i3-tail-EGFP display increased localization of the EGFP labelled portion to the mitochondria, upon serum starvation for 2 hours and incubation of the cells in HBSS buffer, in presence of Mitotracker: **a**, is IRES-driven M_2tail(368-466)-EGFP. **b,** Cap dependent M_2-mRuby2 + IRES-driven M_2tail(368-466)-mRuby2, both derived from the M_2-mRuby2 gene. **c**, Mitotracker Deep Red **d**, Overlay of Mitotracker Deep Red and EGFP channel. **e**, Overlay between GFP and mRuby2. **f-l**, Localization of the mutant construct M_2(M368A)-mRuby2-STOP-M_2-i3-tail-EGFP in HEK293 cells after 2 hours incubation in HBSS buffer. The same legend as in **a-e** applies. Bottom: Schematic structure of the mega constructs M_2(M368A)-mRuby2-STOP-M_2-i3-tail-EGFP. This construct is similar to the M_2-mRuby2-STOP-M_2-i3-tail-EGFP construct but the methionine 368 in the M_2 sequence has been replaced with alanine. The asterisks represent the stop codons at the end of mRuby2 and EGFP. EGFP was excited at 488 nm and fluorescence collected between 500-600 nm; mRuby2 was excited at 561 nm and fluorescence collected between 580-620 nm. Mitotracker deep red was excited at 633 nm and fluorescence collected between 650-650 nm. Scale bars are 10 µm.

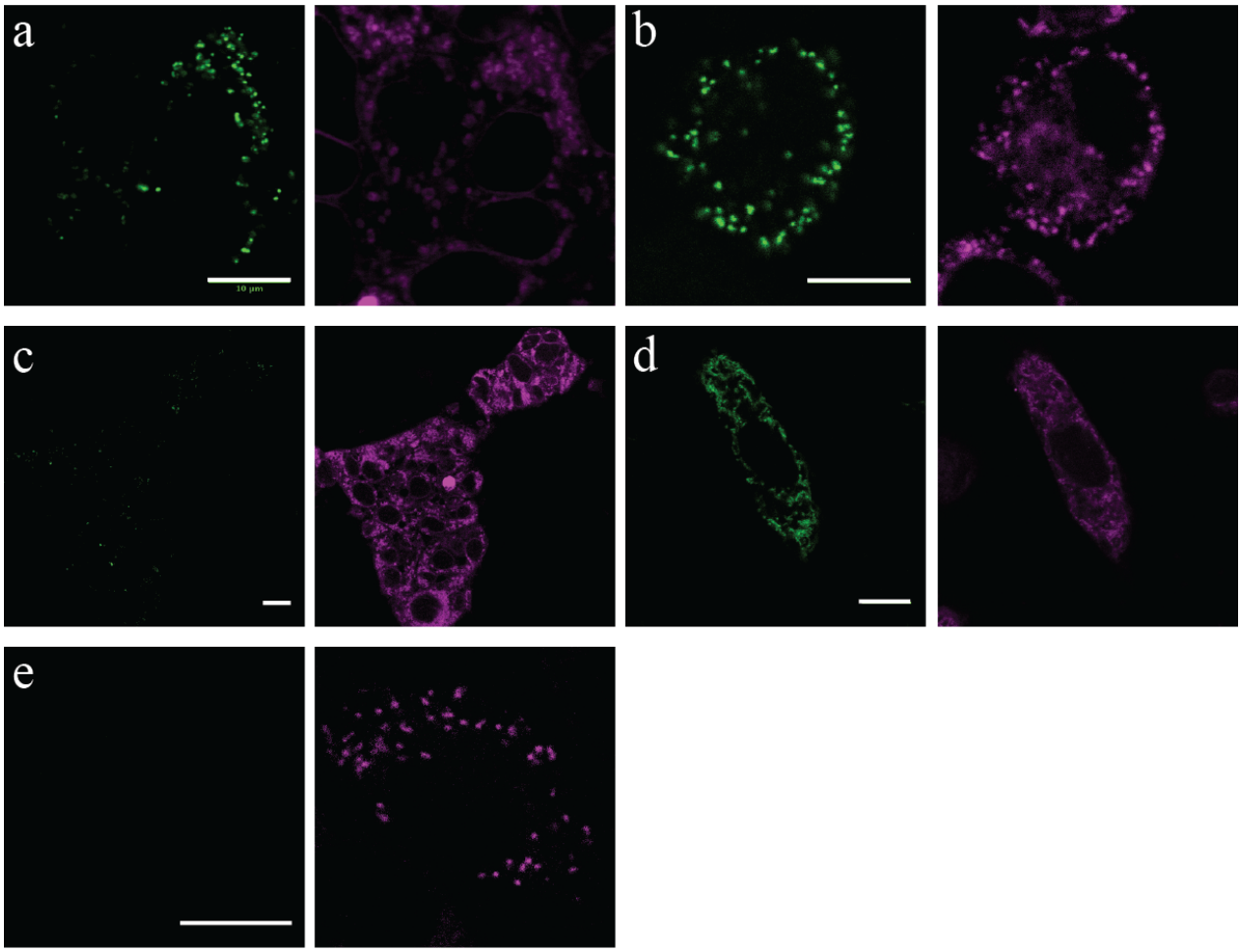

Supp. Fig. 13. Cellular localization of split GFP constructs in HEK293 cells. Confocal micrographs of **a,** co-expression of SMAC-GFP11 and SMAC-GFP1-10 (positive control) and corresponding Mitotracker deep red image. **b,** mito-GFP11 and mito-GFP1-10 (positive control). **C,** M_2tail(368-466)-GFP11 and SMAC-GFP1-10. **D,** M_2tail(368-466)-GFP11 and mito-GFP1-10. **e,** mito-GFP1-10 alone (negative control). EGFP was excited at 488 nm and fluorescence collected between 500-600 nm. Mitotracker deep red was excited at 633 nm and fluorescence collected between 650-650 nm. Scale bars are 10 µm.

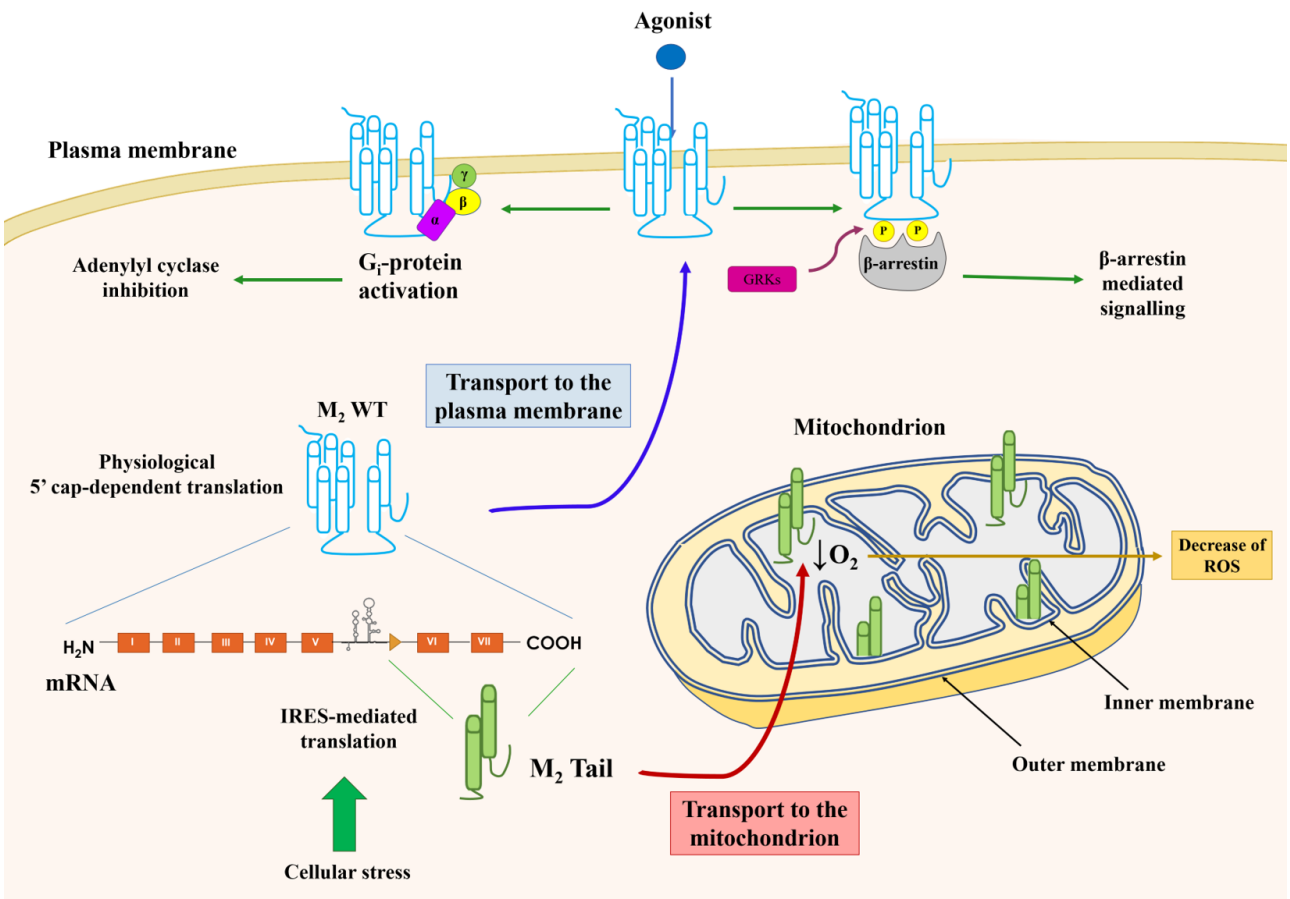

Fig. 6. Schematic representation of the wild type M_2 receptor gene products, their destination in the cell and their function. The M_2 receptor gene give rise to two different transcripts: when translation starts from the canonical cap site the wild type M_2 receptor is generated (in blue). When translation is driven by the internal ribosome entry site (IRES) the C-terminal fragment M_2tail is generated (in green). The two proteins are then sorted in two different cell compartments where they play completely different roles: the M_2 receptor is transported to the plasma membrane where it functions as a G protein-coupled neurotransmitter receptor and inhibits the adenylyl cyclase and β-arrestin mediated signalling. The M_2tail is instead transported in the mitochondria where it inhibits mitochondrial respiration and reduces ROS formation. IRES driven M_2tail translation is probably stimulated in para-physiological and pathological conditions and might have a protective role in cells expressing muscarinic M_2 receptors.

Methods

Statistical analysis. Significance values reported in the graphs, in comparing tabulated values, were determined by a one-tailed Student t-test using Prism 9 (GraphPad Software), and significance values (p-values) are indicated according to the following legend: **** $p<0.0001$; *** $0.0001<p<0.001$; ** $0.001<p<0.01$; * $0.01<p<0.05$. p-values larger than 0.05 are deemed non-significant. Unless otherwise indicated, bar charts and scatter plots indicate average value with s.e.m.

Generation of mutant muscarinic M_2 receptors. Multiple receptor mutants were constructed starting from the human M_2 muscarinic receptor expressed in the pcD vector [36]. The constructs are sketched in **Supplementary Fig. 1**. The two expression plasmids referred as M_2trunk(1-283) (containing transmembrane domains I-V and the N-terminal portion of the third cytoplasmic loop) and M_2tail(281-466) (containing transmembrane domains VI and VII, and the C-terminal portion of the third cytoplasmic loop) were described previously [12].

M_2stop228 – This plasmid was created by substituting codon 228 (CAA) with a stop codon (TAA) at the N-terminal of the i3 loop of the wild type M_2 receptor.

M_2stop228/stop400 – This plasmid was created by inserting an additional stop codon – TGG was substituted with TAA – at the position codon 400 of the TM region VI of the M_2stop228 mutant.

M_2stop400 – This plasmid was created by substituting codon 400 (TGG) with a stop codon (TAA) in the TM region VI of the wild type M_2 receptor.

M_2stop196 – This plasmid was created by substituting codon 196 (TAT) with a stop codon (TAA) in the TM region V of the wild type M_2 receptor.

M_2stop196/stop400 – This plasmid was created by inserting an additional stop codon in the TM region VI of the M_2stop196 mutant, where TGG was substituted with TAA at position of the codon 400.

M_2stop228/fr.sh. – This plasmid was created by inserting four bases (AATT) fifteen nucleotides downstream of the stop codon to create a shift in the correct reading frame of the M_2stop228 mutant.

M_2stop228/hairpin – This construct was created by inserting a 42 bases long sequence (AGGGGCGCGTGGTGGCGGCTGCAGCCGCCACCACGCGCCCC). fifteen nucleotides downstream of the stop codon of the M_2stop228 mutant. Upon transcription, this palindromic sequence has been shown to form a hairpin structure with a ΔG value of −64 kcal/mol that blocks effectively ribosome scanning [37,38].

M_2stop228/stop248, M_2stop228/stop296 and M_2stop228/stop368 – These three constructs were obtained by substituting the three in-frame ATG codons (1. ATG 248, 2. ATG 296 and 3. ATG 368) with the stop codon TAA downstream of the stop228 of the M_2stop228 mutant.

M_2trunk(1-228) – This plasmid was created by substituting codon 228 (CAA) with a stop codon (TAA) at the N-terminal of the i3 loop of the wild type M_2 receptor followed by removal of the downstream sequence.

M_2tail(368-466) – This construct was created by removing all bases of the M_2 receptor sequence up to codon 368 (ATG) of the C-terminal of the i3 loop. The resulting plasmid encodes for a polypeptide fragment that contains the trans-membrane domains VI and VII along with the C-terminal portion of the third cytoplasmic loop.

M2(M368A) – In this construct the third in-frame methionine of the i3-loop of the M_2 muscarinic receptor (ATG) was mutated to alanine (GCG).

M_2-Myc, M_2stop228-Myc, M_2stopM368A-Myc, M_2tail(368-466)-Myc and M_2stop40-Myc – M_2-Myc was purchased from OriGene. This plasmid encodes the human M_2 receptor with a Myc (tag at the C-terminus of the protein. M_2stop228-Myc was obtained by replacing the 0.9 Kb BmtI-PspOMI fragment of the M_2stop228 mutant with

the corresponding fragment of M_2-Myc. M_2stop400-Myc was obtained by substituting the codon 400 (TGG) with a stop codon (TAA) of the M_2-Myc. All the constructs have an additional DDK tag after the C-Myc. Subsequently, all C-Myc constructs were extracted by PCR and subcloned into a bicistrionic pVitro2-MCS plasmid (Invivogen), allowing for the expression of a reporter gene (in our case the red fluorescent protein mRuby2) after an IRES sequence, in order to check for transfection efficiency.

Generation of bicistronic constructs expressing Sirius and EGFP proteins (Fig. 3a).

Sirius[PacI-M_2i3(685-1101)]EGFP – This bicistronic construct was created by inserting the i3 loop of the muscarinic M_2 receptor, from nucleotide 685 to nucleotide 1101, between the ultramarine fluorescent protein (Sirius) and the green fluorescent protein (EGFP). Eight nucleotides corresponding to the recognition site of the PacI enzyme were inserted between Sirius and the i3 loop of the wild type M_2 receptor to alter the reading frame downstream of the Sirius stop codon. Hereafter this plasmid is referred to as Sirius-M_2i3(417n)-EGFP.

Sirius[PacI-M_2i3(685-699)-Hairpin-G]EGFP – This bicistronic construct was created by inserting a 42 nucleotides hairpin loop (see above) between Sirius and the EGFP fluorescent protein. The hairpin loop was spaced from the Sirius stop codon by inserting a PacI recognition sequence and 15 nucleotides of the M_2 i3 loop sequence comprised between nucleotide 685 and nucleotide 699. A G nucleotide was also inserted following the 42 nucleotides of the hairpin loop and upstream of the initial ATG triplet of the EGFP to restore a correct reading frame. Throughout the text we referred to this plasmid as Sirius-H-EGFP.

Sirius[PacI-M_2i3(685-699)-Hairpin-G-PacI-M_2i3(685-1101)]EGFP – This bicistronic construct was created by adding 417 nucleotides of the i3 loop of M_2 from

nucleotide 685 to nucleotide 1101 to the plasmid *Sirius[PacI-M_2i3(685-699)-Hairpin-G]EGFP*. An additional PacI restriction site was also inserted upstream of this segment of the i3 loop. Throughout the text we referred to this plasmid as Sirius-H-M_2i3(417n)-EGFP.

Sirius[PacI-M_2i3(685-699)-Hairpin-G-PacI-M_2i3(685-699/1072-1101)]EGFP – This bicistronic construct was created by deleting from the plasmid *Sirius[PacI-M_2i3(685-699)-Hirpin-G-PacI-M_2i3(685-1101)]EGFP* 372 nucleotides of the M_2 i3 loop, from nucleotide 700 to nucleotide 1071. Throughout the text we referred to this plasmid as Sirius-H-M_2i3(15n/30n)-EGFP.

Sirius[PacI-M_2i3(685-699)-Hirpin-G-PacI-M_2i3(685-699)]EGFP – This bicistronic construct was created by adding 15 nucleotides of the i3 loop of M_2 from nucleotide 685 to nucleotide 699 to the plasmid *Sirius[PacI-M_2i3(685-699)-Hirpin-G]EGFP*. An additional PacI restriction site was also inserted upstream of this short segment of the i3 loop. Throughout the text we will refer to this plasmid as Sirius-H-M_2i3(15n)-EGFP.

Sirius[PacI-M_2i3(685-699)-Hirpin-G-PacI-M_2i3(685-1071)]EGFP – This bicistronic construct was created by adding 387 nucleotides of the i3 loop of M_2 form nucleotide 685 to nucleotide 1071 to the plasmid *Sirius[PacI-M_2i3(685-699)-Hirpin-G]EGFP*. An additional PacI restriction site was also inserted upstream this long segment of the i3 loop. Throughout the text we will refer to this plasmid as Sirius-H-M_2i3(387n)-EGFP.

Mutants of the Sirius-H-M_2i3(15n/30n)-EGFP plasmid – Based on the sequence alignment of amine and adenosine GPCRs, several conserved nucleotides were mutated in order to define the putative IRES sequence. These mutants are reported in **Fig. 3b**.

The fluorescence intensities of the two spectral bands were quantified by the use of a fluorometer and the EGFP intensity values normalized to those of Sirius.

Constructs for fluorescence microscopy.

M_2-EGFP – The wild type M_2 muscarinic receptor was cloned into the pEGFP-N1 expression cassette, between the restriction sites HindIII and XbaI.

M_2-mRuby2 – The wild type M_2 muscarinic receptor was cloned into the mRuby2 vector (Addgene plasmid #40260).

M_2tail(368-466)-EGFP – The M_2tail(368-466)-EGFP was constructed so that the receptor protein would start from the third in-frame methionine of the M_2 i3 loop (M368). The EGFP gene was fused C-terminally following a short restriction site sequence (TCTAGA) of the XbaI enzyme.

M_2tail(368-466)-mRuby2 – The M_2tail(368-466)-mRuby2 was constructed so that the receptor protein would start from the third in-frame methionine of the M_2 i3 loop (M368). The mRuby2 gene was fused C-terminally following a short restriction site sequence (TCTAGA) of the XbaI enzyme.

M_2-mRuby2-STOP-M_2-i3-tail-EGFP – This mega construct was obtained by fusing two preceding constructs, M_2-mRuby2 and M_2tail(368-466)-EGFP, in a unique plasmid, but the M_2tail started at codon 229 (M_2tail(229-466)-EGFP). After the stop codon of mRuby2 and before the codon 229 of M_2tail was inserted a short restriction site sequence (TCCGGA) of the BspEI enzyme (**Fig. 4**).

M_2(M368A)-mRuby2-STOP-M_2-i3-tail-EGFP – This mega construct is analogous to *M_2-mRuby2-STOP-M_2-i3-tail-EGFP, but* the third in-frame methionine of the i3-loop of the M_2 muscarinic receptor was mutated to alanine (M368A) (**Supplementary Fig. 12**).

M_2fr.sh-EGFP – A single base insertion (G) upstream of nucleotide 1102 of the wild type M2 receptor, just before the third in-frame methionine of the i3-loop (M368), induces a frame shift that, following 2 aminoacids, generates a stop codon (TAA) in the amino acid position 370 of the new reading frame. The construct is then fused to EGFP.

M_2fr.sh-mRuby2 – As above, but the EGFP is replaced by a mRuby2.

M_2-GFP11 – A short peptide 16 aminoacids long from the GFP protein, GFP11, was fused to the C-terminus of the muscarinic M_2 receptor. GFP11 was custom syntethised and inserted as a linker between the XbaI and XhoI restriction sites in the plasmid backbone of M_2-EGFP.

Mito-GFP1-10 – The mitochondrial targeting sequence of the cytochrome c oxidase subunit 8A (COX8A) was fused to the N-terminal of GFP1-10 fragment of GFP. GFP1-10 was purchased from Addgene as Addgene plasmid 70219.

Mito-GFP11 – The mitochondrial targeting sequence of COX8A was fused to GFP11 fragment. Mito sequence was obtained from Addgene plasmid 23348.

SMAC-GFP1-10 – The mitochondrial targeting sequence of the SMAC protein was fused to the N-terminal of GFP1-10 fragment. SMAC was obtained from Addgene plasmid 40881.

SMAC-GFP11 – The mitochondrial targeting sequence of the SMAC protein was fused to GFP11 fragment.

M_2tail(368-466)-GFP1-10 – The GFP1-10 fragment was fused to the C-terminus of the muscarinic M_2tail(368-466) receptor fragment.

M_2tail(368-466)-GFP11 – The GFP11 fragment was fused to the C-terminus of the muscarinic M_2tail(368-466) receptor fragment.

Constructs for in-vitro mitochondrial import assays

PSP64-M_2tail(368-466)-5Met - The vector backbone PSP64 (courtesy of Ruaridh Edwards). The following primers: FWD: ATGATGTAAtctagaggaggcggacgc, REV: CATCATCATccttgtagcgcctatgttcttataatg were used to add five methionines to the C-terminal domain of the M_2tail(368-466)-GFP11 template (see above) using Q5® Site-Directed Mutagenesis Kit (New England Biolabs® Inc.). The construct was then extracted with appropriate restriction enzymes (HindIII and XbaI) and ligated into the vector backbone PSP64 (courtesy of Ruaridh Edwards).

PSP64-M2R-5Met – The following primers: FWD: ATGATGTAAtctagaggaggcggacgc REV: CATCATCATccttgtagcgcctatgttcttataatg were used to add five methionines to the C-terminal domain of to the M_2-GFP11 template (see above) using Q5® Site-Directed Mutagenesis Kit (New England Biolabs® Inc.). The construct was then extracted with appropriate restriction enzymes (HindIII and XbaI) and ligated into the vector backbone PSP64.

All constructs were sequenced either with a Genetic Analyzer 3500 (Applied Biosystem®) or by a professional sequencing service (LGC Genomics, Berlin).

Reverse transcription. Reverse transcription was performed using a 24-nucleotide antisense oligo (TTACCTTGTAGCGCCTATGTTCTT) directed against the last 24 nucleotides at the 3' end of the M_2 open reading frame. cDNA amplification was carried out with the same antisense oligo used for reverse transcription, together with a 24 nucleotides sense oligo (ATGAATAACTCAACAAACTCCTCT) directed against the first 24 nucleotides at the 5' end of the M_2 open reading frame.

Cell culture and transfection. COS-7 (African green monkey kidney fibroblast-like SV40 transformed cell line) and CHO (Chinese Hamster Ovary) cells (from American Type Culture Collection) were grown at 5% CO_2 and 37 °C, in high glucose Dulbecco's modified Eagle's medium (DMEM) supplemented with 10% fetal bovine serum (FBS), 2 mM L-glutamine, 50 IU/ml penicillin, and 50 mg/ml streptomycin, and non-essential amino acids. HeLa cells (from American Type Culture Collection) were cultured in the same medium, but with the double amount of L-glutamine. SHSY-5Y cells were cultured in Roswell Park Memorial Institute (RPMI) medium supplemented with 10% FBS, 2 mM L-glutamine, 50 IU/ml penicillin, and 50 mg/ml streptomycin. Media and reagents used for cell cultures were from Euroclone, PAN Biotech, Biochrome and Sigma-Aldrich. Cell transfection was performed using FuGene® transfection reagents (Promega) as recommended by the manufacturer. Eighty percent confluent cells were washed twice with free-serum medium and the mix of FuGene and plasmid DNA was added. In every experimental condition 6-8 µg of plasmid DNA per Petri (10 cm^2) were used. Cells were grown for 48 h post-transfection before use. In co-transfection experiments, half amount of each plasmid DNA was used. All microscopy experiments were performed with transiently transfected HEK293 (Human Embryonic Kidney, ECACC 96121229 from Sigma-Aldrich Chemie GmbH) and COS-7 cells. HEK293 cells were cultured in DMEM (Dulbecco's modified Eagle's medium PAN biotech, Aidenbach, Germany), supplemented with 4.5 g/L Glucose, 2 mM L-Glutamine, 10% FCS, 100 units/mL penicillin and 0.1 mg/mL streptomycin and maintained at 37 °C and 5% CO_2. Cells cultured in 15-cm dishes were split at a 1:36 ratio into 6-well plates containing poly-D-lysine (PDL)-coated 24 mm glass coverslips. Cells were transfected using Effectene transfection reagent (QIAGEN) according to the manufacturer's instructions. Cells seeded on PDL-coated coverslips in 6-well plates were transfected 16 hours after seeding with 0.6 µg plasmid/well.

Fluorescence microscopy. Fluorescence microscopy experiments were performed either on a Leica SP5 (or SP8) Confocal Microscopes, using HyD photon counting detectors and an Argon/Ion laser (or white light laser) source for 488 nm/633 nm excitation and a solid-state diode laser (or white light laser) for 561 nm excitation. A solid-state diode laser was used for 405 nm excitation. A 40x 1.3 NA objective was used, and the electronic zoom was set to achieve a pixel size of 50 nm. For visualization, mitochondria of transfected cells were labelled for 30 minutes at 37 C with 50nM MitoTracker® Deep Red FM (Invitrogen™, Thermo Scientific).

Ligand binding studies. Cells were lysed 48 h post-transfection with ice-cold 2 mM EDTA, 1 nM Na-HEPES (pH 7.4), scraped with a rubber policeman in the presence of ~4 ml rinsing medium, and homogenized with a Polytron homogenizer (ULTRA-TURRAX) in binding assay buffer (50 mM Tris-HCl, pH 7.4, 155 mM NaCl, 0.01 mg/ml bovine serum albumin). Radioligand bindings were carried out at 37 °C for 3 h in a final volume of 1 ml. Non-specific binding was determined in presence of 1 μM atropine. For competition binding assays, increasing concentrations of carbachol (from 0.01 μM up to 10 μM) were used in presence of 200 pM [^{3}H]N-Methylscopolamine ([^{3}H]NMS; 78.9 Ci/mmol; PerkinElmer).

The bound ligand was separated from the unbound ligand using glass-fiber filters (Whatmann, GF/B) with a Brandel Cell Harvester, and filters were counted with a scintillation β-counter. K_D values of [^{3}H]NMS were calculated in direct saturation experiments, whereas carbachol Inibitory Concentration $(IC)_{50}$ values were calculated in competition curves, against 400 pM [^{3}H]NMS, fitted to one binding models using the iterative, non-linear least-squares regression analysis of OriginPro 7.5 software (OriginLab Corporation).

Phosphatidylinositol Breakdown Assay. Transfected COS-7 cells were incubated with myo-[^{3}H]inositol (23 Ci/mmol; PerkinElmer) for 48 h. Immediately before the experiment the cells were washed twice with phosphate-buffered saline and incubated for 15 min in Eagle's medium

containing 10 mM LiCl and 20 mM HEPES. The medium was then replaced by 0.25 ml of the same medium containing the experimental agents. After a 1-hour incubation at 25 °C the reaction was arrested by the addition of 0.75 ml of 7.5% (w/v) ice-cold trichloroacetic acid followed by a 30-min incubation on ice. The trichloroacetic acid was extracted with water-saturated diethyl ether (3 × 4 ml), and levels of IP_1 determined by anion exchange chromatography.

Adenyl Cyclase Assay. COS-7 cells were transfected with plasmid(s) containing the receptor of interest plus adenyl cyclase V. 24 h after transfection the cells were detached with trypsin and re-cultured in 24-well plates. Following an additional period of 24 h culture, they were assayed for adenyl cyclase activity. The assay was performed in triplicate**.** In brief, cells were incubated in 24-well plates for 2 h with 0.25 ml/well of fresh growth medium containing 5 μCi/ml [^{3}H]adenine (PerkinElmer). The medium was then replaced with 0.5 ml/well of DMEM containing 20 mM HEPES, pH 7.4, 0.1 mg of bovine serum albumin, and the phosphodiesterase inhibitors 1-methyl-3-isobutylxanthine (0.5 mM) and Ro-20–1724 (0.5 mM). AC activity was stimulated by the addition of 1 μM forskolin in the presence or absence of carbachol. After 10 min of incubation at +30 °C the medium was removed, and the reaction terminated by addition of perchloric acid containing 0.1 mM unlabeled cAMP followed by neutralization with KOH. The amount of [^{3}H]cAMP formed under these conditions was determined by a two-step column separation procedure (referenza?).

Immunoblot of muscarinic M_2 receptor mutants transfected in HEK293 cells. Cells were seeded in 10 cm plates and transfected after 24h according to manufacturer protocols (Effectene, Qiagen) using 2 μg of plasmid DNA. 48h after transfection cells were washed (2x) in ice cold PBS. 200 μL per plate of ice-cold lysis buffer were added. Lysis buffer was a RIPA buffer: 50 mM Tris-HCL pH 8, 150 mM NaCl, 1% TRITON, 0.5% sodium deoxycholate and

0.1% SDS. The following compounds were added to the buffer to a final 1x dilution: 100x Halt Protease Inhibitor Cocktail (Thermo Fisher), 100x 0.5 M EDTA and (10x) 10 mM PMSF. Cells were then scraped and the cell lysate transferred to pre-cooled 1.5 mL Eppendorf tubes. The tubes were placed in a Thermomixer at 4 °C, 300 rpm for 30 minutes. Then the Eppendorf tubes were centrifuged for 30 minutes at 14000 rpm at 4 °C. The supernatant was then transferred to new Eppendorf tubes. Protein concentration in the cell lysates was quantified by a BCA assay (Pierce BCA Protein Assay Kit, from Thermo Fisher) according to manufacturer instructions.

Cell lysates were loaded into 10% polyacrylamide gels. Cell lysates were loaded using Laemmli Buffer 2x (Sigma Aldrich) in equal mass. As a reference marker we loaded 5 uL of PageRuler Prestained Protein Ladder (Thermo Fisher). Gels were mounted into a Mini Protean Tetra Cell kit (BioRad) using 1x SDS running buffer. Gels were ran using a constant voltage of 90V for approximately 15 minutes, and afterwards at 130V for 45 minutes. Gels were transferred to PVDF membranes. Wet transfer was achieved by using the Mini Trans Blot Module (BioRad) in Wet Transfer Buffer (25 mM Tris pH 8.3, 192 mM Glycine and 20% MetOH) at 350 mA for 90 minutes. The immunoblotted membranes were then blocked in 5% Milk in TBS-T for 1 hour at room temperature. The membrane was then incubated overnight at 4 °C with primary antibody solution using the following concentrations depending on the antibody used: 1:1000 anti **β**-actin (13E5) rabbit primary antibody (Cell Signaling), 1:1000 anti myc-Tag (9B11) mouse primary antibody (Cell Signaling). After overnight incubation, the membranes were washed 3x 10 minutes in TBS-T and incubated at RT for 1 h with a secondary antibody (1:10000 anti-mouse IgG/(anti rabbit) HRP-linked antibody from Cell Signaling).

After the incubation with the secondary antibody, the membrane was washed 3x 10 minutes in TBS-T. Detection was achieved by eliciting HRP luminescence by incubating the membrane with SuperSignal WestFemto solution (Thermo Fisher) according to the manufacturer's instructions, and imaging the membrane using a c600 Transilluminator from Azure Biosystems.

Animal Experiments. All animal experiments were carried out according to the German animal welfare act, considering the guidelines of the National Institute of Health and the 2010/63/EU Directive of the European Parliament on the protection of animals used for scientific purposes. The animals had free access to food and water and were kept in individually ventilated cages under a 12h:12h light/dark regime (light from 6:30 am to 6:30 pm), a constant 22±2°C temperature and 55±10% humidity.

The transgenic line B6.Cg-Chrm2tm1.1Hze/J, also known as Chrm2-tdT-D knock-in, was obtained from 'The Jackson Laboratory' (Stock No: 030330). They are heterozygous animals, designed to have expression of a Chrm2/tdTomato fusion protein directed by the endogenous M2 muscarinic acetylcholine receptor promoter/enhancer sequences.

Tissue preparation and immunoblot of endogenous M_2 receptor in Chrm2-tdT-D knock-in mice. Mouse tissues were weighed out and ice-cold lysis buffer was added to approx. 0.2-0.5mg tissue/ml buffer (10mM K2HPO4, 150mM NaCl, 5mM EDTA, 5mM EGTA, 1% Triton X-100, 0.2% Na-deoxycholate. Fresh protease inhibitors PMSF 0.5mM, Na3VO4 0.1mM, NaF 50mM, Jenny's mix (Soybean trypsin inhibitor 3.2µg/ml, Aprotinin 2µg/ml, Benzamidin 0.5mM) were added to the buffer.

Samples were first homogenized, and then pellet debris were centrifuged at 4°C for 30 minutes at max speed (tabletop) and the supernatant (soluble proteins) was transferred into fresh tube (pellets = non-soluble proteins)

Protein concentration were determined with BCA assay. Cell lysates were loaded using Laemmli Buffer 2x (Sigma Aldrich) in equal mass (see above for the immunoblot procedure) into 8% polyacrylamide gels.

The membrane was then incubated overnight at 4 °C with primary antibody solution (1:1000 anti **β**-actin (13E5) rabbit primary antibody #4970 from Cell Signaling) (1:1000 anti GAPDH) (1:1000 anti-TdTomato rabbit primary antibody #632496 from Takara).

Isolation of mitochondrial fractions and immunodetection. Cells were seeded in 15 cm plates and transfected after 24h according to manufacturer protocols (Effectene, Qiagen) using 5 µg of plasmid DNA. 48h after transfection cells were harvested and centrifuged at 1000 rpm for 10 minutes, resuspended in NaCl 0.9% (w/v) and centrifuged at 1000 rpm for 10 minutes.
Mouse tissue were freshly excised and placed in ice cold PBS (1x) . The samples were washed with NaCl 0.9% (w/v). The homogenization steps were performed with Precellys Evolution Homogenizer, at 4500 rpm for 10 seconds.
The samples were processed according to manufacturer protocols (Qproteome Mitochondria Isolation Kit, Qiagen). From the different steps were obtained three different fractions: the cytosolic, the microsomal and the mitochondrial fraction.
The fresh mitochondrial pellet was resuspended in 150µL of ice-cold lysis buffer and the protein concentration of the three fractions from each sample was quantified with a BCA assay (see above).
Cell lysates were loaded into 12% polyacrylamide gels using an SDS loading buffer (6x solution: 2.28g Tris-HCl, 2.313 DTT, 6g SDS, 30% Glycerol and 0.03% bromophenol blue in a final volume of 50 mL) in equal mass (see above for the immunoblot procedure).
The membrane was then incubated overnight at 4 °C with primary antibody solution using the following concentrations: 1:1000 anti **β**-actin (13E5) rabbit primary antibody (#4970 from Cell Signaling), 1:1000 anti-tdtomato rabbit primary antibody (#632496 from Takara), 1:1000 anti **β**-tubulin mouse primary antibody, 1:1000 anti GAPDH mouse primary antibody, 1:1000 anti COXIV mouse primary antibody (#ab33985 from abcam).

Quantification of M_2tail(368-466) mitochondrial import kinetics from confocal time sequences. Before imaging, 2.5×10^4 HEK-TSA cells were seeded in each PDL-coated well of the µ-Slide 8 well (Ibidi) with DMEM (ScienCell™) supplemented with 10% FBS and 1% P/S

overnight, and transfected with a total of 2 μg C-terminal EGFP tagged M_2 tail using Lipofectamine 2000 (Thermo Fisher Scientific) according to the manufacturer protocol after washing with 200 μL PBS and refreshing with 100 μL DMEM (ScienCell™) supplemented with 10% FBS and 1% P/S. After transfection for five hours, mitochondria of transfected cells were rapidly labelled with 50nM MitoTracker® Deep Red FM (Invitrogen™, Thermo Scientific) in FluoroBrite DMEM medium (Thermo Scientific) supplemented with 1% P/S for 20 minutes after the removal of old culture medium. After mitochondria labeling, the μ-Slide were washed twice with FluoroBrite DMEM medium (Thermo Scientific) and subsequently mounted onto the TCS SP8 confocal microscope (Leica) (See imaging). Firstly, the stage of the microscope was equilibrated in temperature, and the acquisition mode was set to the tile scanning. After storing the position of each desired transfected cells, the imaging mode was set to XYT and a HC PL APO CS2 40×/NA1.3 oil immersion objective was selected. Both DIC channel and HyD were utilized to obtain 512×512 pixels images. Laser wavelengths were set as described in the section Fluorescence Microscopy above. All settings remained the same throughout the whole measurement. Images were taken at every 30 minutes over a 5h interval. The images were afterwards analyzed by ImageJ software, using the Plugin 'JACoP'. Briefly, the degree of colocalization between EGFP-tagged M_2tail(368-466) (CH1) and MitoTracker stained mitochondria (CH2) was quantified by Mander's colocalization coefficients [39]. The two colocalization coefficients M1 ($M1 = \frac{CHB}{CH1}$) and M2 ($M2 = \frac{CHB}{CH2}$), CHB indicates overlapping pixels in channel 1 and channel 2. A threshold was determined for individual channel in order to distinguish specific signals from nonspecific ones. Due to their sensitivities to thresholds, the Pearson correlation coefficient (PCC)[40], as well as the faster decaying attribute of nonspecific signals, were also taken into account while estimating thresholds for each channel. For the analysis of each cell, the threshold for Mitotracker channel was kept constant. Whereas the threshold for EGFP channel was evaluated based on the PCC value.

Transfection and expression of split-GFP constructs in HEK293 cells. To perform the sequential split GFP complementation assay illustrated in **Figures 4h-i and 5g**, 3×10^5 HEK-TSA cells were seeded on a 10% poly-D-lysine (PDL)-coated 25mm coverslip in each well of a Falcon® 6-well flat-bottom plate (StemCell™) and cultured overnight. Cells were transfected using Effectene (see above) with a 0.4 µg Mito-GFP1-10 plasmid. The cells were then washed once with fresh 2 mL phosphate-buffered saline (PBS) first and supplemented with 1.5 mL fresh DMEM medium (ScienCell™) supplemented with 10% FBS and 1% P/S. After adding the transfection mixture, the cells were cultured overnight. After the first transfection, a second transfection of a 0.6 µg plasmid encoding either the C-terminal GFP11 tagged M_2tail(368-466) or M_2 receptor was performed using the Effectene Transfection Reagent (Qiagen). After washing each well with 2 mL PBS, the old medium was exchanged with 1.5 mL low glucose Minimum Essential Medium (MEM) (Gibco™, Thermo Scientific) supplemented with 1% P/S, in order to create a stress-like cell starvation condition. After a four hours starvation, the cells were fixed using 4% polyformaldehyde (PFA)/PBS at 37°C for 30 minutes and washed twice with PBS before imaging.

Oxygen consumption measured with the Seahorse assay. $5x10^4$ COS7 cells were seeded in seahorse 24MW plates with Complete media (DMEM supplemented with 10%FBS and 1X PS) and then incubated for about 4h at 37C in a cell incubator. After this incubation, cells were washed twice with Seahorse media supplemented with glutamate (1 mM), pyruvate (1 mM) and glucose (20 mM) and then incubated for 1h at 37 °C in an incubator without CO2 before being analyzed in the Seahorse XF Analyzers. In particular, the baseline cell oxygen consumption rate (OCR) was measured at the beginning of the assay, followed by measurements of ATP linked respiration and maximal respiratory capacity after the addition of respectively oligomycine (1 µM) and the FCCP protonophore (1 µM). Finally, rotenone (1 µM), an inhibitor of complex I, and antimycin (1 µM), inhibitor of complex III, were added to shut down

completely the electron transport chain (ETC) function, revealing the non-mitochondrial respiration.

Generation of M368A hiPSC clone. The human induced pluripotent stem cell (hiPSC) line BIHi005-A (https://hpscreg.eu/cell-line/BIHi005-A) was used to generate an isogenic iPSC clone (BIHi005-A-39) with **M368A mutation** using a protocol previously described[41]. In brief, small guide RNA (sgRNA) targeting the M_2 gene close to the mutation site to be corrected were designed using the http://crispor.tefor.net/ webpage and the sgRNA (5`-AGTCATCTTCACAATCTTGC-3`) were synthesized by Integrated DNA technologies (https://eu.idtdna.com). The donor ssODN template was designed to convert the ATG to GCT and was synthesized as an Ultramar DNA oligo by IDT. (5´-AAAAGTGACTCATGTACCCCAACTAATACCACCGTGGAGGTAGTGGGGTCTTCAG GTCAGAATGGAGATGAAAAGCAGAATATTGTAGCCCGCAAGATTGTGAAGGCTA CTAAGCAGCCTGCAAAA-3´). The Ribonucleoprotein (RNP) complexes were prepared by incubating of 1.5µg Cas-9 protein and 360 ng gRNA for 10 minutes at room temperature. For delivery of RNPs and ssODN template, 10µl cell suspension containing Cas9 RNPs and ssODN and 1x105 cells were electroporated using the Neon transfection System (ThermoFisher Scientific). The electroporated cells were plated in one well of 6 well plate with StemFlex media (ThermoFisher Scientific) supplemented CloneR™ (Stemcell technologies). Three days after the transfection we analyzed the bulk population using the Sanger sequencing to estimate the editing efficiency. Thereafter, the automated single cell cloning of the genome edited cell pool was performed as described in protocol [42]. The clones were screened by SANGER sequencing. The positive confirmed clones were banked and characterized for pluripotency and karyotype stability as described in [43].

Briefly, for pluripotency assay, single cells were labelled with conjugated antibodies. Surface markers (SSEA1, SSEA4 and TRA1-60) staining was performed in unfixed cells by incubation with antibodies diluted in 0.5% BSA/PBS (10 min, 4 °C, dark). Intracellular markers (OCT3/4, NANOG) were stained by fixation/permeabilization solution (Miltenyi Biotec, 130-093-142) (30 min, 4 °C, dark) followed by antibody incubation in permeabilization buffer (Miltenyi Biotec) (30 min, 4 °C, dark). Analysis was done using the MACSQuant® AnalyzerVYB and FlowJo v10.4.

Briefly, for karyotype stability, genomic DNA was isolated using the DNeasy blood and tissue kit (Qiagen, Valencia, CA, United States) and samples were analyzed using the human Illumina OMNI-EXPRESS-8v1.6 BeadChip. First, the genotyping was analyzed using GenomeStudio 1 genotyping module (Illumina). Thereafter, KaryoStudio 1.3 (Illumina) was used to perform automatic normalization and to identify genomic aberrations utilizing settings to generate B-allele frequency and smoothened Log R ratio plots for detected regions. The stringency parameters used to detect copy number variations (CNVs) were set to 75 kb (loss), 100 kb (gain) and CN-LOH (loss of heterozygosity) regions larger than 3 MB.

Culture and handling of hiPSCs cells. hiPSCs were cultured on Geltrex (Thermo Fisher) coated plates using: Essential 8 medium (Thermo Fisher). The culture was routinely monitored for mycoplasma contamination using a PCR assay. 10 μM ROCK Inhibitor Y-27632 2HCl (Selleck Chemicals, #SEL-S1049) was added after cell splitting to promote survival. hiPSC cultures were kept in a humidified atmosphere of 5% CO2 at 37°C and 5% oxygen. hiPSCs were undirectedly differentiated to a mixture of three lineages (ectodermal, endodermal and mesodermal) by replacing Essential 8 medium with DMEM-F12 medium supplemented with 10% FBS for seven days. 10 μM ROCK Inhibitor Y-27632 2HCl (Selleck Chemicals) was added after cell splitting to promote survival.

Cell proliferation assay with HEK293 cells. $4x10^5$ HEK293 cells 24h after transfection and $4x10^5$ hPSCs were seeded respectively in T25 flask and pre-coated T25 flask, in culture medium with Atropine at final concentration of 100nM; the medium with Atropine was replaced every day. After 72h from transfection of the HEK293 and from seeding of the hiPSCs, the medium and the cells were collected and centrifuged, the pellet was resuspended in the same amount of medium for each pellet; an aliquots of the resuspension was mixed with the same amount of Trypan blue (ratio 1:1), 10 microliters were used for counting in a Neubauer chamber.

Fluorescence plate reader assays. HEK293 cells were grown on 6 well plates without coverslips, and, upon reaching 60-70% confluence, the cells were transfected using Effectene (Quiagen, Venlo Netherlands) according to the manufacturer's instructions. After 24 h the cells were split and transferred to 96 well (black plate) at a seeding density of 50,000 cells/well. The 96 well plate was pre-coated with Poly-D-Lysine for 30 min at RT. The medium was removed and each well was washed 3x with 100µl HBSS. The cells were finally analyzed by a fluorescence plate reader (Neo2, BioTek, Bad Friedrichshall) in HBSS.

Extracellular oxygen consumption. HEK293 cells 24h after transfection and hPSCs were harvested and seeded respectively in 96 multiwell black plate and pre-coated (Geltrex A1413302, Thermo Fisher) 96 multiwell black plate, $5x10^4$ cells for well; after incubation O/N at 37 °C and in 5% CO2, the cell culture medium was replaced by HBSS and the assay were performed according to the manufacturer protocols (abcam Extracellular Oxygen Consumption Assay).

Author Contributions

PA, FP, IF, ZW, MR, IP, RE, HZ, UZ, MET, JDG, SS, ART, SA conduced primary experiments; MG, CP, GA, FM, BP, AR contributed to the experimental data; NT and SD contributed tools and reagents. PA, IP, IF, MR, UZ, AT, KT, VF, FA, FG, MS contributed to experimental design and assisted in writing paper, PA, MJL and RM conceived and lead the study, and wrote the paper.

Competing Interests

The authors declare that they have no conflicts of interest with the contents of this article.

Data Availability Statement

Source data are provided with this manuscript.

References

1 Kruse, A. C. *et al.* Muscarinic acetylcholine receptors: novel opportunities for drug development. *Nat Rev Drug Discov* **13**, 549-560, doi:10.1038/nrd4295 (2014).

2 Fryer, A. D., Christopoulos A. & Nathanson N.M. in *Handb. Exp. Pharmacol.* Vol. 208 1-499 (2012).

3 Novi, F., Scarselli, M., Corsini, G. U. & Maggio, R. The paired activation of the two components of the muscarinic M3 receptor dimer is required for induction of ERK1/2 phosphorylation. *J Biol Chem* **279**, 7476-7486, doi:10.1074/jbc.M306818200 (2004).

4 Novi, F., Scarselli, M., Corsini, G. U. & Maggio, R. An unusual form of the association binding kinetics of N-[3H]methylscopolamine to the split muscarinic M2trunk/M2tail receptor. *J Pharmacol Exp Ther* **305**, 786-795, doi:10.1124/jpet.102.045393 (2003).

5 Jackson, R. J. & Kaminski, A. Internal initiation of translation in eukaryotes: the picornavirus paradigm and beyond. *RNA* **1**, 985-1000 (1995).

6 Hellen, C. U. & Sarnow, P. Internal ribosome entry sites in eukaryotic mRNA molecules. *Genes Dev* **15**, 1593-1612, doi:10.1101/gad.891101 (2001).

7 Calebiro, D., Nikolaev, V. O., Persani, L. & Lohse, M. J. Signaling by internalized G-protein-coupled receptors. *Trends in Pharmacological Sciences* **31**, 221-228, doi:https://doi.org/10.1016/j.tips.2010.02.002 (2010).

8 Zhang, X., Bedigian, A. V., Wang, W. & Eggert, U. S. G protein-coupled receptors participate in cytokinesis. *Cytoskeleton (Hoboken)* **69**, 810-818, doi:10.1002/cm.21055 (2012).

9 Hebert-Chatelain, E. *et al.* A cannabinoid link between mitochondria and memory. *Nature* **539**, 555-559, doi:10.1038/nature20127 (2016).

10 Suofu, Y. *et al.* Dual role of mitochondria in producing melatonin and driving GPCR signaling to block cytochrome c release. **114**, E7997-E8006, doi:10.1073/pnas.1705768114 %J Proceedings of the National Academy of Sciences (2017).

11 Maggio, R. *et al.* Variants of G protein-coupled receptors: a reappraisal of their role in receptor regulation. *Biochem Soc Trans* **44**, 589-594, doi:10.1042/BST20150239 (2016).

12 Maggio, R., Vogel, Z. & Wess, J. Reconstitution of functional muscarinic receptors by co-expression of amino- and carboxyl-terminal receptor fragments. *FEBS Lett* **319**, 195-200, doi:10.1016/0014-5793(93)80066-4 (1993).

13 Park, P. S. & Wells, J. W. Monomers and oligomers of the M2 muscarinic cholinergic receptor purified from Sf9 cells. *Biochemistry* **42**, 12960-12971, doi:10.1021/bi034491m (2003).

14 Bathe-Peters, M., Gmach, P., Annibale, P. & Lohse, M. J. Linescan microscopy data to extract diffusion coefficient of a fluorescent species using a commercial confocal microscope. *Data Brief* **29**, 105063, doi:10.1016/j.dib.2019.105063 (2020).

15 Dong, C., Filipeanu, C. M., Duvernay, M. T. & Wu, G. Regulation of G protein-coupled receptor export trafficking. *Biochim Biophys Acta* **1768**, 853-870, doi:10.1016/j.bbamem.2006.09.008 (2007).

16 Kamiyama, D. *et al.* Versatile protein tagging in cells with split fluorescent protein. *Nat Commun* **7**, 11046, doi:10.1038/ncomms11046 (2016).

17 Bonfili, L. *et al.* Essential amino acid mixtures drive cancer cells to apoptosis through proteasome inhibition and autophagy activation. *FEBS J* **284**, 1726-1737, doi:10.1111/febs.14081 (2017).

18 Thakor, N. & Holcik, M. IRES-mediated translation of cellular messenger RNA operates in eIF2alpha- independent manner during stress. *Nucleic Acids Res* **40**, 541-552, doi:10.1093/nar/gkr701 (2012).

19 Holcik, M. & Sonenberg, N. Translational control in stress and apoptosis. *Nat Rev Mol Cell Biol* **6**, 318-327, doi:10.1038/nrm1618 (2005).

20 Newman, L. E., Schiavon, C. & Kahn, R. A. Plasmids for variable expression of proteins targeted to the mitochondrial matrix or intermembrane space. *Cell Logist* **6**, e1247939, doi:10.1080/21592799.2016.1247939 (2016).

21 Ishizuka, T., Ozawa, A., Katsuura, M., Nomura, S. & Satoh, Y. Effects of muscarinic acetylcholine receptor stimulation on the differentiation of mouse induced pluripotent stem cells into neural progenitor cells. *Clin Exp Pharmacol Physiol* **45**, 1198-1205, doi:10.1111/1440-1681.12993 (2018).

22 Hoogduijn, M. J., Cheng, A. & Genever, P. G. Functional nicotinic and muscarinic receptors on mesenchymal stem cells. *Stem Cells Dev* **18**, 103-112, doi:10.1089/scd.2008.0032 (2009).

23 Weinberg, Z. Y. & Puthenveedu, M. A. Regulation of G protein-coupled receptor signaling by plasma membrane organization and endocytosis. *Traffic* **20**, 121-129, doi:10.1111/tra.12628 (2019).

24 Jong, Y. I., Harmon, S. K. & O'Malley, K. L. GPCR signalling from within the cell. *Br J Pharmacol* **175**, 4026-4035, doi:10.1111/bph.14023 (2018).

25 Benard, G. *et al.* Mitochondrial CB(1) receptors regulate neuronal energy metabolism. *Nat Neurosci* **15**, 558-564, doi:10.1038/nn.3053 (2012).

26 Lefkimmiatis, K., Leronni, D. & Hofer, A. M. The inner and outer compartments of mitochondria are sites of distinct cAMP/PKA signaling dynamics. *J Cell Biol* **202**, 453-462, doi:10.1083/jcb.201303159 (2013).

27 Marti-Solano, M. *et al.* Combinatorial expression of GPCR isoforms affects signalling and drug responses. *Nature* **587**, 650-656, doi:10.1038/s41586-020-2888-2 (2020).

28 van Heesch, S. *et al.* The Translational Landscape of the Human Heart. *Cell* **178**, 242-260 e229, doi:10.1016/j.cell.2019.05.010 (2019).

29 Pestova, T. V., Shatsky, I. N. & Hellen, C. U. Functional dissection of eukaryotic initiation factor 4F: the 4A subunit and the central domain of the 4G subunit are sufficient to mediate internal entry of 43S preinitiation complexes. *Mol Cell Biol* **16**, 6870-6878, doi:10.1128/mcb.16.12.6870 (1996).

30 Jan, E. & Sarnow, P. Factorless ribosome assembly on the internal ribosome entry site of cricket paralysis virus. *J Mol Biol* **324**, 889-902, doi:10.1016/s0022-2836(02)01099-9 (2002).

31 Fitzgerald, K. D. & Semler, B. L. Bridging IRES elements in mRNAs to the eukaryotic translation apparatus. *Biochim Biophys Acta* **1789**, 518-528, doi:10.1016/j.bbagrm.2009.07.004 (2009).

32 Ingolia, N. T., Hussmann, J. A. & Weissman, J. S. Ribosome Profiling: Global Views of Translation. *Cold Spring Harb Perspect Biol* **11**, doi:10.1101/cshperspect.a032698 (2019).

33 Zhang, J., Nuebel, E., Daley, G. Q., Koehler, C. M. & Teitell, M. A. Metabolic regulation in pluripotent stem cells during reprogramming and self-renewal. *Cell Stem Cell* **11**, 589-595, doi:10.1016/j.stem.2012.10.005 (2012).

34 Guo, C., Sun, L., Chen, X. & Zhang, D. Oxidative stress, mitochondrial damage and neurodegenerative diseases. *Neural Regen Res* **8**, 2003-2014, doi:10.3969/j.issn.1673-5374.2013.21.009 (2013).

35 Kritsiligkou, P. *et al.* Unconventional Targeting of a Thiol Peroxidase to the Mitochondrial Intermembrane Space Facilitates Oxidative Protein Folding. *Cell Rep* **18**, 2729-2741, doi:10.1016/j.celrep.2017.02.053 (2017).

36 Bonner, T. I., Buckley, N. J., Young, A. C. & Brann, M. R. Identification of a family of muscarinic acetylcholine receptor genes. *Science* **237**, 527-532, doi:10.1126/science.3037705 (1987).

37 Kozak, M. Constraints on reinitiation of translation in mammals. *Nucleic Acids Res* **29**, 5226-5232, doi:10.1093/nar/29.24.5226 (2001).
38 Kozak, M. Circumstances and mechanisms of inhibition of translation by secondary structure in eucaryotic mRNAs. *Mol Cell Biol* **9**, 5134-5142, doi:10.1128/mcb.9.11.5134 (1989).
39 Manders, E. M. M., Verbeek, F. J. & Aten, J. A. Measurement of Colocalization of Objects in Dual-Color Confocal Images. *J Microsc-Oxford* **169**, 375-382, doi:DOI 10.1111/j.1365-2818.1993.tb03313.x (1993).
40 Manders, E. M. M., Stap, J., Brakenhoff, G. J., Vandriel, R. & Aten, J. A. Dynamics of 3-Dimensional Replication Patterns during the S-Phase, Analyzed by Double Labeling of DNA and Confocal Microscopy. *J Cell Sci* **103**, 857-862 (1992).
41 Richardson, C. D., Ray, G. J., DeWitt, M. A., Curie, G. L. & Corn, J. E. Enhancing homology-directed genome editing by catalytically active and inactive CRISPR-Cas9 using asymmetric donor DNA. *Nat Biotechnol* **34**, 339-344, doi:10.1038/nbt.3481 (2016).
42 Vallone, V. F. *et al.* Methods for Automated Single Cell Isolation and Sub-Cloning of Human Pluripotent Stem Cells. *Curr Protoc Stem Cell Biol* **55**, e123, doi:10.1002/cpsc.123 (2020).
43 Metzler, E., Telugu, N., Diecke, S., Spuler, S. & Escobar, H. Generation of two human induced pluripotent stem cell lines derived from myoblasts (MDCi014-A) and from peripheral blood mononuclear cells (MDCi014-B) from the same donor. *Stem Cell Res* **48**, 101998, doi:10.1016/j.scr.2020.101998 (2020).